

UC Berkeley

SEMM Reports Series

Title

Formulation and Numerical Analysis of an Anisotropic Damage Model with a Localized Dissipative Mechanism

Permalink

<https://escholarship.org/uc/item/5vz3j1bs>

Author


Armero, Francisco

Publication Date

1997-05-01

**REPORT NO.
UCB/SEMM-97/11**

**STRUCTURAL ENGINEERING
MECHANICS AND MATERIALS**



**FORMULATION AND NUMERICAL ANALYSIS OF
AN ANISOTROPIC DAMAGE MODEL WITH A
LOCALIZED DISSIPATIVE MECHANISM**

BY

F. ARMERO

MAY 1997

**DEPARTMENT OF CIVIL AND ENVIRONMENTAL ENGINEERING
UNIVERSITY OF CALIFORNIA, BERKELEY**

Formulation and Numerical Analysis of an Anisotropic Damage Model with a Localized Dissipative Mechanism

by

F. ARMERO

Structural Engineering, Mechanics and Materials
Department of Civil and Environmental Engineering
University of California, Berkeley CA 94720

Abstract

This paper presents the formulation of an anisotropic damage model that incorporates the localized dissipative mechanism associated to the formation of cracks in a brittle material (concrete). This mechanism is characterized as the inelastic work done by the stresses on the singular strains (a delta function) corresponding to the crack displacements. The singularity of these fields in a local neighborhood of a material point is considered in the proposed constitutive model through the formalism of strong discontinuities without smoothing. The model is incorporated in a standard formulation of the equilibrium of the solid (the large-scale problem), involving in particular smooth displacements and strains. This step involves matching the dissipation observed in the large-scale problem with the dissipation of the proposed local model. It is shown that this methodology leads to a well-defined formulation. Furthermore, the finite element implementation of the proposed formulation arises naturally in the context of the enhanced strain finite element methods. The proposed method involves no regularization of the discontinuities and leads to mesh size independent solutions. Connections with traditional smeared crack methods are identified at this numerical level. Representative numerical simulations involving general unstructured meshes are presented.

1. Introduction

The failure of brittle materials is characterized by the formation and propagation of cracks in the material. While the response of the cracked solid softens with further loading, a degraded (damaged) response is observed upon unloading. The highly oriented character of this phenomenon leads to an anisotropic response of the damaged solid. Furthermore, the final collapse of the solid is often precluded by the formation of highly localized patterns of the deformation, in the form of localization bands. A characteristic example is cracking of concrete in tension. It is the goal of this paper to formulate and implement numerically a

model of anisotropic damage that simulates correctly these particular aspects of the failure of brittle materials.

Local continuum formulations based on a rate-independent stress/strain relation are known to lead to ill-posed problems when strain-softening is considered, due to a change of type of the governing equations (loss of ellipticity). See the classical analyses of HILL [1962] and MANDEL [1966], and the recent complete analyses in RICE [1976], OTTOSEN & RUNESSON [1991], and NEILSEN & SCHREYER [1993], among others. The main difficulty can be traced to the modeling of the localized dissipative mechanisms that appear in the final stages of the deformation of the solid. In brittle materials, this localized dissipative mechanism can be characterized by the stress/crack-displacement softening cohesive laws governing the formation and propagation of cracks, as originally proposed in BARENBLATT [1962] extending the approach of DUGDALE [1960] for ductile materials. See also KACHANOV [1986] for the incorporation of continuum damage. The energy is dissipated per unit area of created fracture surface (rather than per unit volume), leading to non-physical solutions if a stress/strain softening law is assumed. At the numerical level, these deficiencies lead to the well-known pathological dependence on the mesh size of finite element solutions based on a local continuum with rate-independent strain-softening.

Finite element approaches accommodating directly stress/displacement relations were introduced in HILLERBORG et al [1976] and HILLERBORG [1984] with the so-called *discrete crack approach*. However, given that typical practical applications require the solution of large-scale problems, it is of the main interest to maintain the local continuum framework of the model and its numerical implementation. Furthermore, this framework is known to characterize very well the pre-failure response of the material. These reasons have motivated the search of alternative approaches to overcome the difficulties associated to a local continuum with strain-softening.

Smearred crack models are commonly employed in the analysis of brittle materials as it is the interest of this paper. See e.g. BAZANT & OH [1983], ROTS et al [1985], or the more recent review of KROPLIN & WEIHE [1997], among many others. These models are based on the introduction of the so-called “crack strains” as a smeared measure of the accumulated crack displacements in a finite element. A stress-strain softening law is then introduced, but such that it leads to the proper energy dissipation distributed over the volume of the finite element. The dependence of the softening modulus on the element size is then concluded, through the so-called characteristic length (see e.g. PIETRUSZCZAK & MRÓZ [1981], and OLIVER [1989]). The constitutive model is then intricately related with the finite element formulation: *the mechanical model depends on the numerical implementation through the mesh size*. As described below, this relation is studied in detail herein.

Alternative regularization approaches involve the change of the simple local continuum framework to introduce explicitly a characteristic length in the constitutive model. Typical examples are non-local models (BAZANT et al [1984]), models based on Cosserat continua

(DEBORST & SLUYS [1991]), and higher-gradient models (COLEMAN & HODGON [1985]). A difficulty often associated to these models is the definition (and actual determination) of the length parameter as a material parameter. For practical purposes, the solution of the non-local or higher order partial differential equations that appear in these formulations (with the corresponding boundary conditions in the internal variable fields) is sometimes difficult to motivate. This concern is especially important when we note again the different scales involved in the problem, and if the solution of the large-scale system is the primary interest. The approaches that incorporate the characteristic lengths of the fine scales require, in particular, their numerical resolution, a task that may become overwhelming in its computational cost, if not impossible, for typical practical applications.

Motivated by these observations, we have presented recently a number of analyses based on the consideration of strong discontinuities. See SIMO, OLIVER & ARMERO [1993] for an analysis of these solutions and their relation with a localized dissipative mechanism. As presented in detail in ARMERO & GARIKIPATI [1996] for finite strain multiplicative plasticity, a bifurcation analysis allows to identify the consistency of a localized softening mechanism with classical inelastic continuum models. See also the exposition in OLIVER [1996] and the approach presented in LARSSON & RUNESSON [1996]. Numerical implementations have been presented in these references, involving, in particular, the consideration of the strong discontinuities without regularization (smoothing), as proposed in ARMERO & GARIKIPATI [1995]. See also the related approach presented in DVORKIN et al. [1990]. Implementations involving regularized strong discontinuities can be found in SIMO, OLIVER & ARMERO [1993].

The formulation of anisotropic damage models has received an important amount of attention in the literature. The works presented in CORDEBOIS & SIDOROFF [1982], ORTIZ [1985], SIMO & JU [1987] and references therein, are representative examples. In this paper we present the formulation and numerical implementation of an anisotropic damage model for brittle materials with the strong discontinuities as the starting point. More specifically, it is shown that the consideration of a set of localized internal variables (including the compliance of the crack) with a formalism based on distribution theory leads to the formulation of an objective model, in the sense that the correct dissipation of the energy (i.e., per unit area and not per unit volume) is accomplished. The model assumes the formation of the crack in mode I. The damage evolution equations are obtained through the principle of maximum damage dissipation (see SIMO & JU [1987]). These considerations are made in a local neighborhood of a material point, the so-called small scales. The resulting model incorporates directly the stress/crack-displacement laws obtained experimentally, without the smearing or smoothing of the discontinuities.

Our main goal is the development of a large-scale model involving the smooth fields of standard formulations of the mechanical boundary value problem, given its appropriateness for numerical implementations. The inclusion of meso- and micro- mechanical effects in large scale analyses (multi-scale analyses) is nowadays an area of intensive research (see

e.g. FISH & BELSKY [1995], and references therein). Similarly, the recent contribution of HUGHES [1996] identifies a multi-scale approach as a common setting for the numerical analysis of several problems in computational mechanics. This recent interest motivates in part the presentation in this paper.

In this context, the proposed anisotropic model developed locally in a neighborhood of a material point (the small scale) is incorporated in a weak formulation of the standard mechanical boundary value problem, exhibiting, in particular, smooth solutions. The “bridge” is built by equating the dissipation observed in both problems. Similar to the so-called enhanced strain formulation of SIMO & RIFAI [1990] for the development of improved finite element methods, the (smooth) large-scale problem is enhanced with the singular strains arising from the strong discontinuities, the unresolved strains. The consideration of the limit problem as the measure of the assumed neighborhood tends to zero allows to identify the consistency of the proposed formulation with the standard local continuum framework. In addition, it is shown that this methodology defines completely the different fields appearing in the problem. The final numerical implementation of these considerations fits then in the framework of the enhanced strain finite element method. No special regularization of the discontinuities is required. The explicit modeling of the localized softening response along the crack results in solutions independent of the mesh size exhibiting the correct localized dissipation.

In contrast with previous smeared crack models, the proposed mechanical constitutive model incorporates the localized effects of the cracks in the material without relying on a numerical regularization (smearing). The local model is formulated in the traditional local continuum framework with the help of distribution theory, without requiring the introduction of ad-hoc characteristic lengths at this constitutive level. It is next, through the “bridging” procedure described above linking these local and large-scale problems, that the role played by the length scales commonly used in smeared formulations is fully characterized. In particular, this procedure identifies a connection between traditional smeared crack formulations and more sound anisotropic damage models.

We emphasize again that the model developed in this work is understood as a *large-scale* model, capturing correctly (objectively) the dissipative effects of the small scales, but treating the small length scales as unresolvable otherwise. The local continuum framework is maintained, leading to efficient numerical methods of analysis of the pre- and post-failure states of the large-scale structural systems of interest in this work. At this numerical level, the localized dissipative effects are resolved locally at the element level by the assumed enhanced part of the strain field. Special interpolations of the local fields are shown to lead to traditional smeared crack formulations, up to the treatment of the shear response of the cracks.

An outline of the rest of the paper is as follows. Section 2 describes the equations defining the mechanical boundary value problem, the so-called large scale problem. Section 3 includes the developments leading to the anisotropic damage model. Complete details

characterizing the energy dissipation in the model through the incorporation of stress-displacement relations are included. The connection between the two problems is established in Section 4, through the so-called “equi-dissipation bridge”. The proposed model is analyzed and shown to recover consistently the local continuum framework. Next, we describe in Section 4.2 the enhanced strain finite element formulation that implements the above considerations. Section 5 depicts the solution obtained with the proposed formulation in representative numerical simulations. Section 6 concludes with some final remarks.

2. The Large-Scale Problem

We summarize in this section the equations governing the mechanical boundary value problem of interest in this work. Regardless of the details particular to the constitutive model defined in Section 3, the equations for the large-scale problem as assumed in this section retain the usual regularity properties of, e.g., linear elasticity. Standard results regarding the definition of the traction vector are summarized in Section 2.2.

2.1. The governing equations

Consider a domain $\Omega \subset \mathbb{R}^{n_{\text{dim}}}$ ($n_{\text{dim}} = 1, 2$ or 3) defining the reference placement of a solid body \mathcal{B} , identified with its current placement under the assumption of infinitesimal strains assumed hereafter. As noted in the introduction, it is our goal to formulate a large-scale model involving the standard continuum framework. To this purpose, we begin with the introduction of the space of admissible (large-scale) displacement variations

$$\mathcal{V} = \left\{ \boldsymbol{\eta} : \Omega \rightarrow \mathbb{R}^{n_{\text{dim}}} : \boldsymbol{\eta} = 0 \quad \text{on} \quad \partial_{\mathbf{u}}\Omega \right\}, \quad (2.1)$$

that is, satisfying homogeneous boundary conditions on $\partial_{\mathbf{u}}\Omega$ where the displacement field is imposed. The functions $\boldsymbol{\eta} \in \mathcal{V}$ are assumed smooth, in the sense that $\mathcal{V} \subset H^1(\Omega)$, with the standard notation for the Sobolev space $H^1(\Omega)$ of functions with square integrable $L_2(\Omega)$ derivatives.

Following the introduction of the space \mathcal{V} in (2.1), we define the affine space of admissible large-scale displacements as

$$\mathcal{S} := \{ \mathbf{u} : \Omega \rightarrow \mathbb{R}^{n_{\text{dim}}} : \mathbf{u} = \mathbf{g} + \mathbf{w}, \text{ for some } \mathbf{w} \in \mathcal{V} \}. \quad (2.2)$$

Here, \mathbf{g} is a smooth function such that

$$\mathbf{g} = \bar{\mathbf{g}} \quad \text{on} \quad \partial_{\mathbf{u}}\Omega, \quad (2.3)$$

for an imposed displacement $\bar{\mathbf{g}}$ on $\partial_{\mathbf{u}}\Omega$, so we have

$$\mathbf{u} = \bar{\mathbf{g}} \quad \text{on} \quad \partial_{\mathbf{u}}\Omega \quad \forall \mathbf{u} \in \mathcal{S}, \quad (2.4)$$

i.e., satisfaction of the essential boundary conditions is assumed for the displacement fields in \mathcal{S} , as usual. The infinitesimal *large-scale strains* are then obtained as

$$\boldsymbol{\varepsilon}(\mathbf{u}) := \nabla^s \mathbf{u} := \frac{1}{2} [\nabla \mathbf{u} + (\nabla \mathbf{u})^T] , \quad (2.5)$$

with components in $L_2(\Omega)$ as a consequence of the assumed regularity of the displacement field \mathbf{u} in (2.2). The usual symbol $(\cdot)^T$ has been employed in (2.5) to denote the matrix transpose.

Let $\boldsymbol{\sigma} = \boldsymbol{\sigma}(\mathbf{x}) \in \mathbb{R}^{n_{\text{dim}} \times n_{\text{dim}}}$ (symmetric) be the stress field in equilibrium with a body force $\mathbf{f} : \Omega \rightarrow \mathbb{R}^{n_{\text{dim}}}$ and imposed tractions $\bar{\mathbf{t}} : \partial_T \Omega \rightarrow \mathbb{R}^{n_{\text{dim}}}$ acting on the part $\partial_T \Omega \subset \partial \Omega$ of the boundary of the solid. The usual assumptions

$$\partial_u \Omega \cap \partial_T \Omega = \emptyset \quad \text{and} \quad \overline{\partial_u \Omega \cup \partial_T \Omega} = \partial \Omega , \quad (2.6)$$

in each of the n_{dim} components of the displacement/traction are considered for a well-posed problem.

The large-scale problem in $\mathbf{u} \in \mathcal{S}$ is finally determined with the consideration of the weak form of the equilibrium equations of the solid Ω . In the quasi-static limit, the governing equations read

The Large Scale Problem. Find $\mathbf{u} \in \mathcal{S}$ satisfying

$$\int_{\Omega} \boldsymbol{\sigma} : \nabla^s \boldsymbol{\eta} \, d\Omega = \int_{\Omega} \mathbf{f} \cdot \boldsymbol{\eta} \, d\Omega + \int_{\partial_T \Omega} \bar{\mathbf{t}} \cdot \boldsymbol{\eta} \, d\Gamma \quad \forall \boldsymbol{\eta} \in \mathcal{V} , \quad (2.7)$$

where the stress field $\boldsymbol{\sigma}$ is a function of the the strains $\boldsymbol{\varepsilon}(\mathbf{u})$ and other internal variables as characterized by the constitutive model developed in the following section. □

The starting regularity assumption $\mathcal{V} \subset [H^1(\Omega)]^{n_{\text{dim}}}$ reiterates again our goal to formulate the large-scale problem in Ω under the standard framework of, e.g., infinitesimal elasticity (see e.g. MARSDEN & HUGHES [1983], Section 6.1) or hardening plasticity (see JOHNSON [1978]). To make mathematical sense of the left-hand-side of (2.7), the stress field is assumed to have components in $L_2(\Omega)$, giving the standard regularity to the stress field. The usual assumptions of smooth loading and domain are considered for simplicity (see MARSDEN & HUGHES [1983] for a discussion). The motivation behind these particular choices for the regularity of each field arises from the tools of analysis available. In particular, the assumed large-scale fields can be easily resolved by standard techniques of finite element analyses of the problem, as illustrated in Section 4.2. Additional contributions due to the specific response of the material (e.g., discontinuities) are introduced as discussed in Section 3.

2.2. The traction vector

A standard argument based on the weak form (2.7) of the equilibrium equations shows the continuity of tractions for a given orientation defined by a unit vector \mathbf{n} . Indeed, let Γ be a generic smooth surface passing through a point $\mathbf{x} \in \Omega$ with normal \mathbf{n} . Let Ω^+ and Ω^- each of two connected components in which the domain Ω is divided

Assume that the stress field $\boldsymbol{\sigma}$ exhibits the added regularity of having components in $[C^1(\bar{\Omega}^+)] \cup [C^1(\bar{\Omega}^-)]$, i.e., with continuous first derivatives. Integration by parts of (2.7) under this assumption, and accounting for the internal surface Γ with unit normal \mathbf{n} leads to

$$\begin{aligned} \int_{\Omega \setminus \Gamma} [\operatorname{div} \boldsymbol{\sigma} + \mathbf{f}] \cdot \boldsymbol{\eta} \, d\Omega + \int_{\Gamma} [[\boldsymbol{\sigma}]] \mathbf{n} \cdot \boldsymbol{\eta} \, d\Gamma \\ + \int_{\partial_T \Omega} [\bar{\mathbf{t}} - \boldsymbol{\sigma} \mathbf{n}] \cdot \boldsymbol{\eta} \, d\Gamma = 0 \quad \forall \boldsymbol{\eta} \in \mathcal{V}, \end{aligned} \quad (2.8)$$

where $[[\boldsymbol{\sigma}]]$ denotes the jump in the stress field across Γ . A standard argument leads then the strong form of the equilibrium equations and natural boundary conditions,

$$\operatorname{div} \boldsymbol{\sigma} + \mathbf{f} = 0 \quad \text{in } \Omega \setminus \Gamma, \quad (2.9)$$

$$\boldsymbol{\sigma} \mathbf{n} = \bar{\mathbf{t}} \quad \text{on } \partial_T \Omega, \quad (2.10)$$

together with the local form of the equilibrium across Γ given by

$$[[\boldsymbol{\sigma}]] \mathbf{n} = 0. \quad (2.11)$$

Therefore, we have the well-defined vector

$$\mathbf{T}_\Gamma := \boldsymbol{\sigma} \mathbf{n} \Big|_\Gamma, \quad (2.12)$$

for all directions \mathbf{n} , where the restriction at $\mathbf{x} \in \Gamma \subset \Omega$ is understood in this last formula. We shall refer to the vector \mathbf{T} as the traction vector on Γ at $\mathbf{x} \in \Omega$ for the orientation \mathbf{n} in the large-scale.

Remark 2.1. The argument leading to the pointwise definition (2.12) of the traction vector relies on the added C^1 smoothness of the stress field. The argument extends to general $L_2(\Omega)$ stress fields by the continuity of the different terms in (2.7) involving $L_2(\Omega)$ stresses and strains, with the appropriate trace operator on the surface Γ . See DE VITO [1966]. \square

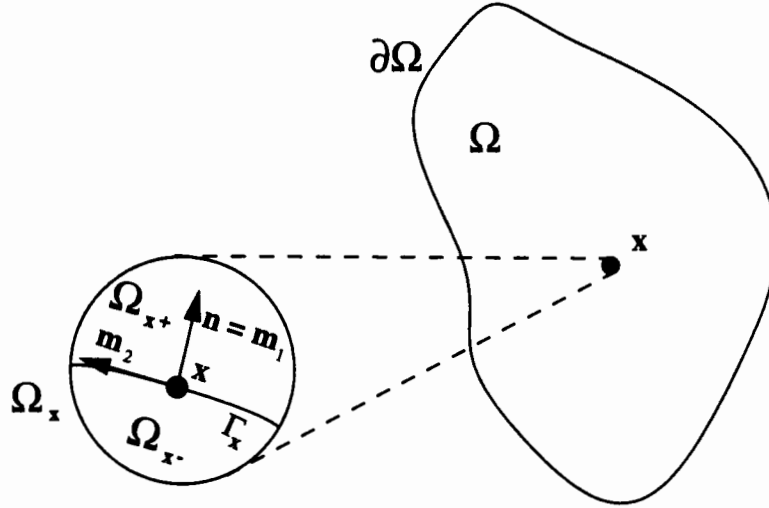


FIGURE 3.1. Definition of the neighborhood $\Omega_x \subset \Omega$ at a material point \mathbf{x} , with the smooth surface Γ_x and the corresponding orthogonal reference system $\{\mathbf{m}_1 \equiv \mathbf{n}, \dots, \mathbf{m}_{n_{\text{dim}}}\}$ ($n_{\text{dim}} = 2$ in the figure).

3. Characterization of Localized Anisotropic Damage Mechanisms

The formulation of the damage model is described in this section. The previous section introduced the large-scale problem leaving undefined the constitutive relation between the stress and the strain fields. The assumed regularity of the large-scale displacements and corresponding strains may not incorporate all the effects observed in the material response. In the case of interest, these effects correspond to the discontinuities and the corresponding localized dissipation due to the appearance of cracks in the material.

In this context, the kinematics of strong discontinuities and singular internal variables characterizing the localized damage due to the formation of cracks in the material is described in this section. The main goal is to determine the constitutive relation for the stress field that incorporates the proper (objective) localized damage mechanisms.

3.1. The crack displacements and the unresolved strains

The stress field $\boldsymbol{\sigma} = \boldsymbol{\sigma}(\mathbf{x})$ has been introduced in Section 2. To define its relation to the deformation of the solid in a certain point $\mathbf{x} \in \Omega$, consider a neighborhood $\Omega_x \subset \Omega$ whose dimensions and full characterization will be detailed in Section 4. The arguments in the rest of this section take place in this *fixed neighborhood* Ω_x . This neighborhood can be thought as a “magnifying lens” that allows us to consider the “*small scale effects*” of the response of the material; see Figure 3.1. While looking through this lens, we concentrate on the fields in the neighborhood Ω_x without imposing a-priori any compatibility requirements with the fields observed by considering a different material point $\mathbf{x} \in \Omega$. The incorporation of these effects in the large-scale problem defined in Section 2 is accomplished in Section 4.

The interest herein is focused on a brittle solid characterized by a tensile strength f_t under mode I fracture. Assume that a crack forms at the material point $\mathbf{x} \in \Omega$ with unit normal \mathbf{n} , the maximum principal stress direction corresponding to the principal stress reaching the tensile strength f_t . Consider a smooth surface $\Gamma_x \subset \Omega_x$ passing through \mathbf{x} and with unit normal \mathbf{n} at \mathbf{x} . The discontinuous displacement field across the crack can be written *locally in* Ω_x using the decomposition

$$\mathbf{u}_\mu(\mathbf{y}) = \mathbf{u}(\mathbf{y}) + \boldsymbol{\xi}(\mathbf{y}) M_{\Gamma_x}(\mathbf{y}) \quad \mathbf{y} \in \Omega_x, \quad (3.1)$$

where the function $M_{\Gamma_x} : \Omega_x \rightarrow \mathbb{R}$ is smooth in $\Omega_x \setminus \Gamma_x$ and has been normalized to have a unit jump discontinuity across Γ_x , that is,

$$[[M_{\Gamma_x}]] = 1 \quad \text{on } \Gamma_x. \quad (3.2)$$

Let H_{Γ_x} denote the Heaviside function across Γ_x , defined by

$$H_{\Gamma_x}(\mathbf{y}) = \begin{cases} 1 & \mathbf{y} \in \Omega_{x+}, \\ 0 & \mathbf{y} \in \Omega_{x-}, \end{cases} \quad (3.3)$$

where Ω_{x+} and Ω_{x-} denote each of the two connected components of the neighborhood Ω_x defined by Γ_x ; see Figure 3.1. Given the definition (3.3) of the Heaviside function, the function M_{Γ_x} can be written

$$M_{\Gamma_x} = H_{\Gamma_x} + N_x, \quad (3.4)$$

for some smooth function N_x .

We introduce the space of displacement jumps

$$\mathcal{J} = \{\boldsymbol{\xi} : \Omega_x \rightarrow \mathbb{R}^{n_{\text{dim}}}\}, \quad (3.5)$$

assumed smooth functions in Ω_x . With these considerations the jump across Γ_x is given by

$$[[\mathbf{u}_\mu]] = \boldsymbol{\xi}. \quad (3.6)$$

Even though the main physical significance of the displacements $\boldsymbol{\xi}$ are the jump across Γ_x , we consider their extension in the neighborhood Ω_x . Details on the structure of the neighborhood Ω_x and the space \mathcal{J} of displacements jumps are presented in Section 4.1.1. The displacement field $\mathbf{u}_\mu : \Omega_x \rightarrow \mathbb{R}^{n_{\text{dim}}}$ defines the displacements observed locally in the small scale around the material point \mathbf{x} , incorporating the localized effects of the crack.

The infinitesimal strains corresponding to the displacement (3.1) are given by

$$\boldsymbol{\varepsilon}_\mu := \nabla^s \mathbf{u}_\mu = \underbrace{\boldsymbol{\varepsilon}(\mathbf{u}) + (\boldsymbol{\xi} \otimes \nabla N_x)^s}_{\text{regular distribution}} + \underbrace{\nabla^s \boldsymbol{\xi} H_{\Gamma_x} + (\boldsymbol{\xi} \otimes \mathbf{n})^s \delta_{\Gamma_x}}_{\text{singular distribution}} \quad \text{in } \Omega_x, \quad (3.7)$$

where the superscript s denotes the symmetric part. The singular part is expressed in terms of the Dirac delta δ_{Γ_x} across Γ_x , a singular distribution using standard terminology in distribution theory. See STAKGOLD [1979] (page 100) for the mathematical details involved in the derivation of (3.7) from (3.1). We introduce the notation

$$\bar{\epsilon}_\mu := \epsilon(\mathbf{u}) + (\boldsymbol{\xi} \otimes \nabla N_{\Gamma_x})^s + \nabla^s \boldsymbol{\xi} H_{\Gamma_x} \quad \text{in } \Omega_x, \quad (3.8)$$

for the regular part of ϵ_μ , and the singular strains

$$\tilde{\epsilon}_\delta := (\boldsymbol{\xi} \otimes \mathbf{n})^s \quad \text{in } \Omega_x. \quad (3.9)$$

With this notation, the strains (3.7) in Ω_x are given by

$$\epsilon = \bar{\epsilon}_\mu + \tilde{\epsilon}_\delta \delta_{\Gamma_x}. \quad (3.10)$$

Alternatively, the total strains ϵ_μ in Ω_x can be decomposed as

$$\epsilon_\mu = \epsilon(\mathbf{u}) + \underbrace{\bar{\epsilon}_{unres} + \tilde{\epsilon}_\delta \delta_{\Gamma_x}}_{:= \epsilon_{unres}}. \quad (3.11)$$

where

$$\bar{\epsilon}_{unres} := \bar{\epsilon}_\mu - \epsilon(\mathbf{u}) = \mathbf{G}(\boldsymbol{\xi}), \quad (3.12)$$

with

$$\mathbf{G}(\boldsymbol{\xi}) = (\boldsymbol{\xi} \otimes \nabla N_{\Gamma_x})^s + \nabla^s \boldsymbol{\xi} H_{\Gamma_x} \quad \text{in } \Omega_x, \quad (3.13)$$

for a linear operator $\mathbf{G}(\cdot)$ of the displacement jump $\boldsymbol{\xi}$. The singular part $\tilde{\epsilon}_\delta$ is also a linear function of $\boldsymbol{\xi}$ by (3.9). Physically, the strain field ϵ_{unres} is the part of the strains in Ω_x which are *unresolved* by the strains $\epsilon(\mathbf{u})$ considered in the large-scale problem. The decomposition (3.11) identifies the regular and singular part of these unresolved strains,

$$\boxed{\epsilon_{unres} = \mathbf{G}(\boldsymbol{\xi}) + (\boldsymbol{\xi} \otimes \mathbf{n})^s \delta_{\Gamma_x}}. \quad (3.14)$$

in terms of the crack displacements $\boldsymbol{\xi}$.

As noted in the introduction, the main goal in the present model is to capture the dissipative effects of the singular fields observed in the small scales of the material, while solving the large-scale problem of interest. The decomposition (3.1) is introduced only as a motivation for the particular form of the total strains (3.11) defined only in Ω_x . The rest of the arguments that follow require only the consideration of this decomposition of the strains. In this way, the operator $\mathbf{G}(\cdot)$ is left unknown a priori. Section 4.1.1 identifies this operator through a consistency argument connecting the large and local problems as $measure(\Omega_x) \rightarrow 0$, collapsing the neighborhood Ω_x to \mathbf{x} .

Remarks 3.1.

1. The local decomposition (3.7) in a regular and a singular part is characteristic of the so-called *strong discontinuity* approach as presented in SIMO, OLIVER & ARMERO [1993], ARMERO & GARIKIPATI [1996], and OLIVER [1996]. In the context presented herein, this approach characterizes the response of the solid locally in Ω_x under the considered assumptions of a brittle material. We note that no compatibility requirements between the displacement fields \mathbf{u} and \mathbf{u}_μ are imposed a-priori on the local decomposition (3.1). See the discussion in the end of Section 4.1.1 below for further comments in this respect.
2. Clearly, the actual choice of what is considered the large and the local fields is arbitrary. For instance, the consideration of smooth large-scale displacement without including the discontinuous part due to the local effects is a particular choice in the formulation. This choice is motivated by the numerical analysis of the problem as developed in Section 4.1.2 below. Whereas the resolution of smooth displacement fields is readily available using standard finite element interpolations, the incorporation of the singular strain fields that appear in the problem require the special considerations developed in this paper. \square

3.2. The crack compliances

Denote by \mathbf{D} the compliance of the material relating the stress field $\boldsymbol{\sigma}$ and the strains $\boldsymbol{\varepsilon}_\mu$, that is, we introduce the relation

$$\boldsymbol{\varepsilon}_\mu = \mathbf{D}\boldsymbol{\sigma} \quad \text{in } \Omega_x, \quad (3.15)$$

defining \mathbf{D} . Given the regularity of the stresses assumed in Section 2 and, in particular, the continuity of tractions as given by (2.12), together with the singular distributional character of the strains as given by (3.7)

$$\boldsymbol{\varepsilon}_\mu = \underbrace{\bar{\boldsymbol{\varepsilon}}_\mu}_{\text{regular distribution}} + \underbrace{\tilde{\boldsymbol{\varepsilon}}_\delta \delta_{\Gamma_x}}_{\text{singular distribution}} = \mathbf{D} \underbrace{\boldsymbol{\sigma}}_{\text{regular distribution}}, \quad (3.16)$$

we obtain the decomposition

$$\boxed{\mathbf{D} = \bar{\mathbf{D}} + \tilde{\mathbf{D}} \delta_{\Gamma_x}}, \quad (3.17)$$

in a regular and a singular part, to make sense of the relation (3.16) by identifying the regular and singular parts of each side of this relation. This result is a consequence of the Lebesgue decomposition theorem (see e.g. ROYDEN [1988], page 278). Physically, the singular part $\tilde{\mathbf{D}}$ of (3.17) defines a localized compliance along the discontinuity Γ_x , the *crack compliances*. Inserting (3.17) in (3.16) and equating singular parts, we conclude

$$\tilde{\boldsymbol{\varepsilon}}_\mu = \tilde{\mathbf{D}}\boldsymbol{\sigma} \quad \text{in } \Omega_x \setminus \Gamma_x, \quad (3.18)$$

and

$$\tilde{\boldsymbol{\epsilon}}_\delta = \tilde{\boldsymbol{D}}\boldsymbol{\sigma} \quad \text{on } \Gamma_x, \quad (3.19)$$

for the singular part corresponding to the crack.

Let \mathbf{m}_i ($i = 2, n_{\text{dim}}$) denote unit vectors such that $\{\mathbf{m}_1 \equiv \mathbf{n}, \dots, \mathbf{m}_{n_{\text{dim}}}\}$ defines an orthonormal system in $\mathbb{R}^{n_{\text{dim}}}$; see Figure 3.1. We introduce the notation

$$\boldsymbol{\xi} = \xi_i \mathbf{m}_i, \quad (3.20)$$

(summation implied over repeated indices) for the crack displacements ξ_i in the local orthonormal basis $\{\mathbf{m}_i\}$. In this notation, the ξ_1 corresponds to the so-called *crack opening displacement* (COD). The singular strains $\tilde{\boldsymbol{\epsilon}}_\delta$ in (3.7) can then be expressed as

$$\tilde{\boldsymbol{\epsilon}}_\delta := (\boldsymbol{\xi} \otimes \mathbf{n})^s = \xi_i \mathbf{P}_i, \quad (3.21)$$

where

$$\mathbf{P}_i := (\mathbf{m}_i \otimes \mathbf{n})^s, \quad (3.22)$$

with the superscript s denoting again the symmetric part.

Given the special form of the left-hand-side of (3.19), as given by (3.21), and assuming symmetry of the compliance, we conclude that the singular compliance tensor $\tilde{\boldsymbol{D}}$ can be written as

$$\tilde{\boldsymbol{D}} = \tilde{D}_{ij} \mathbf{P}_i \otimes \mathbf{P}_j, \quad (3.23)$$

with $\tilde{D}_{ij} = \tilde{D}_{ji}$ ($i, j = 1, n_{\text{dim}}$). With these considerations, equation (3.19) can be written as

$$\boxed{\xi_i = \tilde{D}_{ij} T_j}, \quad (3.24)$$

for $i = 1, n_{\text{dim}}$, where we have introduced the traction vector $\mathbf{T} = T_i \mathbf{m}_i$ in the small scale Ω_x , satisfying

$$\int_{\Omega_x} \boldsymbol{\sigma} : (\boldsymbol{\gamma} \otimes \mathbf{n})^s \delta_{\Gamma_x} d\Omega_x = \int_{\Gamma_x} \mathbf{T} \cdot \boldsymbol{\gamma} d\Gamma_x \quad \forall \boldsymbol{\gamma} \in \mathcal{J}. \quad (3.25)$$

Equation (3.24) defines a relation between the crack displacements and crack stresses, in terms of the crack compliances whose evolutions are obtained in the following section.

3.3. The localized crack dissipation

To derive the equations describing the evolution of the crack compliances $\tilde{\boldsymbol{D}}$ identified in the previous section, we consider a common thermodynamic argument based on the principle of maximum damage dissipation. To this end, we define the intrinsic energy dissipation rate of the stress field $\boldsymbol{\sigma}$ for a strain rate $\dot{\boldsymbol{\epsilon}}_\mu$ in the neighborhood Ω_x as

$$\mathcal{D}_\mu := \int_{\Omega_x} \left[\boldsymbol{\sigma} : \dot{\boldsymbol{\epsilon}}_\mu - \dot{\psi} \right] d\Omega_x, \quad (3.26)$$

that is, as the difference of the stress power associated to the strains $\boldsymbol{\varepsilon}_\mu$ and the rate of change of the free energy

$$\psi = \psi(\boldsymbol{\varepsilon}_\mu; \mathcal{I}) , \quad (3.27)$$

where \mathcal{I} denotes a generic set of internal variables. Superimposed dots denote time derivative, and purely mechanical effects in an isothermal setting are considered. Defining the complementary energy $\chi(\boldsymbol{\sigma}; \mathcal{I})$ by the standard Legendre transform

$$\chi(\boldsymbol{\sigma}; \mathcal{I}) := \max_{\boldsymbol{\varepsilon}_\mu} \{ \boldsymbol{\sigma} : \boldsymbol{\varepsilon}_\mu - \psi(\boldsymbol{\varepsilon}_\mu; \mathcal{I}) \} , \quad (3.28)$$

the dissipation functional (3.26) can be expressed equivalently as

$$\mathcal{D}_\mu = \int_{\Omega_x} [-\dot{\boldsymbol{\sigma}} : \boldsymbol{\varepsilon}_\mu + \dot{\chi}] d\Omega_x , \quad (3.29)$$

in terms of the complementary energy $\chi(\boldsymbol{\sigma}; \mathcal{I})$.

For the case of interest, characterized by the secant compliance of the material \mathbf{D} , the complementary energy (3.28) is given by

$$\chi(\boldsymbol{\sigma}; \mathbf{D}, \alpha) := \frac{1}{2} \boldsymbol{\sigma} : \mathbf{D} \boldsymbol{\sigma} - \mathcal{H}(\alpha) , \quad (3.30)$$

for some potential $\mathcal{H}(\alpha)$, function of the scalar internal variable α characterizing the cohesive softening response of the cracks. The consideration of the secant compliance as internal variables characterizing the damage of the material can be found in ORTIZ [1985] and SIMO & JU [1987]. Given the assumed symmetry of the compliance \mathbf{D} , we conclude that

$$\begin{aligned} \dot{\chi} &= \dot{\boldsymbol{\sigma}} : \mathbf{D} \boldsymbol{\sigma} + \frac{1}{2} \boldsymbol{\sigma} : \dot{\mathbf{D}} \boldsymbol{\sigma} - \frac{d\mathcal{H}}{d\alpha} \dot{\alpha} \\ &= \dot{\boldsymbol{\sigma}} : \boldsymbol{\varepsilon}_\mu + \frac{1}{2} \boldsymbol{\sigma} : \dot{\mathbf{D}} \boldsymbol{\sigma} + q \dot{\alpha} \end{aligned} \quad (3.31)$$

after using the relation (3.15) and introducing the stress-like internal variable q conjugate to α

$$q := -\frac{d\mathcal{H}}{d\alpha} . \quad (3.32)$$

The intrinsic dissipation rate is then obtained as

$$\mathcal{D}_\mu := \int_{\Omega_x} \left[\frac{1}{2} \boldsymbol{\sigma} : \dot{\mathbf{D}} \boldsymbol{\sigma} + q \dot{\alpha} \right] d\Omega_x , \quad (3.33)$$

after (3.29).

We assume that the only damage mechanisms are associated to the discontinuity Γ_x . Assume then

$$\bar{\mathbf{D}} = \mathbf{D}^e = \text{constant} , \quad (3.34)$$

a constant elastic compliance, and

$$\alpha = \tilde{\alpha} \delta_{\Gamma_x} , \quad (3.35)$$

a scalar field localized on the cracks. Combining (3.8), (3.9) and (3.13) with the constitutive equation (3.18), we obtain

$$\bar{\boldsymbol{\varepsilon}}_\mu = \boldsymbol{\varepsilon}(\mathbf{u}) + \mathbf{G}(\boldsymbol{\xi}) = \mathbf{D}^e \boldsymbol{\sigma} \quad \text{in } \Omega_x , \quad (3.36)$$

or equivalently

$$\boldsymbol{\sigma} = \mathbf{C}^e [\boldsymbol{\varepsilon}(\mathbf{u}) + \mathbf{G}(\boldsymbol{\xi})] \quad \text{in } \Omega_x , \quad (3.37)$$

in terms of the elastic compliance \mathbf{D}^e , or alternatively the elastic stiffness moduli $\mathbf{C}^e = \mathbf{D}^{e-1}$. Equation (3.37) relates the stress field with the large-scale strains $\boldsymbol{\varepsilon}(\mathbf{u})$ and the regular part of the unresolved strains $\mathbf{G}(\boldsymbol{\xi})$.

With these assumptions, the intrinsic dissipation rate (3.33) can be written as

$$\mathcal{D}_\mu = \int_{\Omega_x} \tilde{\mathcal{D}}_\mu \delta_{\Gamma_x} d\Omega_x = \int_{\Gamma_x} \tilde{\mathcal{D}}_\mu d\Gamma_x , \quad (3.38)$$

a localized damage dissipation on $\Gamma_x \subset \Omega_x$, with

$$\boxed{\tilde{\mathcal{D}}_\mu := \frac{1}{2} \dot{\tilde{\mathbf{D}}}_{ij} T_i T_j + q \dot{\tilde{\alpha}} = \frac{1}{2} \tilde{\mathbf{D}} : (\mathbf{T} \otimes \mathbf{T}) + q \dot{\tilde{\alpha}} \quad \text{on } \Gamma_x ,} \quad (3.39)$$

identifying the thermodynamical forces $\frac{1}{2}(\mathbf{T} \otimes \mathbf{T})$ and q conjugate to the rate of internal variables $\dot{\tilde{\mathbf{D}}}$ and $\dot{\tilde{\alpha}}$, respectively. The material relation

$$q = q(\tilde{\alpha}) , \quad (3.40)$$

specifies a given cohesive softening relation for the crack opening, derived from the assumed potential $\mathcal{H}(\alpha)$.

We observe that the proposed approach leads effectively to a decoupling of the continuum and localized responses of the material. In this way, the complementary energy function (3.30) can be decomposed as

$$\chi = \bar{\chi}(\boldsymbol{\sigma}) + \tilde{\chi}(\mathbf{T}; \tilde{\mathbf{D}}, \tilde{\alpha}) \delta_{\Gamma_x} , \quad (3.41)$$

in a regular and singular part, with

$$\bar{\chi}(\boldsymbol{\sigma}) = \frac{1}{2} \boldsymbol{\sigma} : \bar{\mathbf{D}} \boldsymbol{\sigma} \quad \text{in } \Omega_x , \quad (3.42)$$

for the regular part, and

$$\tilde{\chi}(\boldsymbol{\sigma}; \tilde{\mathbf{D}}, \tilde{\alpha}) = \frac{1}{2} \tilde{\mathbf{D}} : (\mathbf{T} \otimes \mathbf{T}) - \tilde{\mathcal{H}}(\tilde{\alpha}) \quad \text{on } \Gamma_x , \quad (3.43)$$

for the singular part. This decoupling allows for a separate constitutive modeling of the two different responses of the material, the bulk and the localized response. For simplicity in the present paper, we assume the elastic response for the bulk response. The evolution equations describing localized damage response are developed next.

3.4. The damage evolution equations

The softening response of the localized damage mechanism (crack) can be characterized by n_{surf} damage surfaces $\phi_j(\mathbf{T} \otimes \mathbf{T}, q)$ ($j = 1, n_{surf}$), defined in terms of the thermodynamical forces identified by the expression of the localized dissipation (3.39). The damage evolution equations are obtained through the principle of *maximum damage dissipation*, under the unilateral constraint defined by the damage surfaces

$$\phi_j(\mathbf{T} \otimes \mathbf{T}, q) \leq 0 \quad j = 1, n_{surf}. \quad (3.44)$$

The use of this principle in the derivation of continuum damage models was proposed in SIMO & JU [1987]. In the context of interest herein, consider the dissipation function

$$\begin{aligned} \tilde{\mathcal{L}}_\mu &:= -\tilde{\mathcal{D}}_\mu + \sum_{j=1}^{n_{surf}} \gamma_j \phi_j(\mathbf{T} \otimes \mathbf{T}, q) \\ &= - \left[\frac{1}{2} \dot{\tilde{\mathbf{D}}} : (\mathbf{T} \otimes \mathbf{T}) + q \dot{\tilde{\alpha}} \right] + \sum_{j=1}^{n_{surf}} \gamma_j \phi_j(\mathbf{T} \otimes \mathbf{T}, q), \end{aligned} \quad (3.45)$$

where the *consistency parameters* γ_j are introduced satisfying the Kuhn-Tucker complementary conditions

$$\gamma_j \geq 0, \quad \phi_j \leq 0, \quad \text{and} \quad \gamma_j \phi_j = 0, \quad (j = 1, n_{surf}), \quad (3.46)$$

to enforce the unilateral constraints (3.44). The minimization of $\tilde{\mathcal{L}}_\mu$ for a given rate of the internal variables, $\dot{\tilde{\mathbf{D}}}$ and $\dot{\tilde{\alpha}}$, leads to the following damage evolution equations

$$\left. \begin{aligned} \dot{\tilde{\mathbf{D}}} &= \sum_{j=1}^{n_{surf}} 2 \gamma_j \frac{\partial \phi_j}{\partial (\mathbf{T} \otimes \mathbf{T})}, \\ \dot{\tilde{\alpha}} &= \sum_{j=1}^{n_{surf}} \gamma_j \frac{\partial \phi_j}{\partial q}, \end{aligned} \right\} \quad (3.47)$$

The evolution equations are finally defined with the introduction of the *consistency condition*

$$\gamma_j \dot{\phi}_j = 0 \quad (\text{for } \phi_j = 0), \quad (3.48)$$

($j = 1, n_{surf}$), fully determining together with (3.46) the conditions defining the loading/unloading. Viscous regularizations are easily incorporated in this localized framework. A Perzyna-type regularization (see SIMO & HUGHES [1997], among others) is obtained by replacing the unilateral constraints (3.44), the Kuhn-Tucker (3.46), and consistency conditions (3.48) with the relation

$$\gamma_j = \frac{\langle g(\phi_j) \rangle}{\eta_L}, \quad (3.49)$$

for a scalar function $g(\cdot)$, Macaulay bracket $\langle x \rangle = (x + |x|)/2$, and localized viscous parameter $\eta_L \geq 0$.

The above developments characterize the localized damage mechanism associated to a single crack. The orientation \mathbf{n} of the crack is assumed fixed based on physical considerations. In this respect, the proposed model can be understood as a *fixed crack model*. As the state of stress evolves in a given point, further cracks can be developed at that point. These results are easily extended to the case of multiple cracks, involving the same relations for each crack and leading to the so-called *multiple fixed crack model* (see the review in KROPLIN & WEIHE [1997]). In this context, it is customary the consideration of the so-called *threshold angle*, a minimum angle between opened cracks. The reader is referred to ROTS et al [1985] for further details in the context of smeared crack models.

It is important to emphasize that in contrast with more traditional formulations of continuum anisotropic damage models (like in ORTIZ [1985], SIMO & JU [1987], among others), the proposed formulation involves localized quantities along the discontinuities arising from the cracking of the material. In this respect, the damaged compliances $\tilde{\mathbf{D}}$ (a two rank tensor, not a four rank tensor as in the initial continuum form (3.26)) model clearly the degradation added to the material by the localized effects of the cracks, thus leading to the correct (objective) energy dissipation as discussed in the next section.

As a simple model example, consider the single Mode I damage surface in tension

$$\phi_1 = T_1 + q(\tilde{\alpha}) - f_t \leq 0 \quad (T_1 \geq 0), \quad (3.50)$$

the inequality $\phi_1 < 0$ holding in a closing crack. The damage evolution equations (3.47) read in this case

$$\left. \begin{aligned} \dot{\tilde{\mathbf{D}}}_{11} &= \frac{\gamma_1}{T_1}, \\ \dot{\tilde{\alpha}} &= \gamma_1, \end{aligned} \right\} \quad (3.51)$$

and

$$\dot{\tilde{\mathbf{D}}}_{ij} = 0 \quad \text{for } i, j \neq 1, \quad (3.52)$$

for the different components of the localized compliance $\tilde{\mathbf{D}}_{ij}$ ($i, j = 1, n_{dim}$), together with the Kuhn-Tucker loading/unloading conditions (3.46) and consistency condition (3.48),

with $n_{surf} = 1$. It is common practice in smeared crack models to consider a (constant) degraded shear stiffness via the so-called shear retention factor coefficients (see e.g. ROTS et al [1985]). Similarly, the degradation of the shear response can be accommodated in the model described above through the consideration of constant degraded compliances

$$\tilde{D}_{22} = \tilde{D}_{33} = \tilde{D}_s > 0, \quad (3.53)$$

consistent with the damage evolution equations (3.52). We note that $\tilde{D}_{11} = 0$ initially in the undamaged state, and that no coupling is assumed between the normal and tangential component of the compliance. The main difference between this approach and the shear retention factor of smeared crack models is that (3.53) corresponds to a *stress vs. crack displacement relation*. It can be understood as a regularization of more traditional the smeared crack shear response.

Remark 3.2. As an alternative to the constant degraded shear compliance of the crack (3.53), one may consider the introduction of the damage surfaces in shear, as considered in GOVINDJEE, KAY & SIMO [1995],

$$\phi_j = |T_j| + r_j q - f_j \leq 0 \quad j = 2, n_{dim}, \quad (3.54)$$

where $r_j = f_j/f_t$ for the shear strength $f_j = f_s$, and maintaining $\phi_1 \leq 0$ as defined in (3.50). The corresponding evolution equations read

$$\dot{D}_{11} = \frac{\gamma_1}{T_1}, \quad \dot{D}_{jj} = \frac{\gamma_j}{|T_j|}, \quad \dot{\alpha} = \sum_{j=1}^{n_{dim}} r_j \gamma_j, \quad (3.55)$$

($r_1 = 1$), with the the Kuhn-Tucker conditions (3.46) and consistency condition (3.48) for $j = 1, n_{dim}$. Alternatively, other surfaces can be found in the literature; see e.g. KROPLIN & WEIHE [1997] for an hyperbolic relation between T_1 and T_2 , in the notation employed herein. \square

3.5. The softening law

Relations between the stress components and the crack displacements (the crack opening displacement, COD, and slip) have been used in the literature to characterize completely the response of the crack. The classical work of Hillerborg (see HILLERBORG et al [1976] and HILLERBORG [1984]) is a representative example. See also REINHARDT [1984] for their experimental determination. Smeared crack models effectively incorporate these laws through the so-called crack strains (ROTS et al [1985]) via the introduction of a numerical characteristic length based on the spatial discretization (a measure of the element size). As discussed in Section 1, the introduction of a completely numerical quantity in the formulation of a constitutive model of the material response seems an artificial formalism.

The model developed in the previous sections accommodates naturally these stress vs. crack displacements laws, and the corresponding fracture energy G_f (the area below the curve). In particular, no length parameters were needed. Consider as an example the case characterized by the softening law

$$q(\tilde{\alpha}) = f_t \left(1 - \exp \left[\frac{\tilde{H}}{f_t} \tilde{\alpha} \right] \right), \quad (3.56)$$

for a softening parameter $\tilde{H} < 0$, $\tilde{\alpha} \in [0, \infty)$, and the simple Mode I damage surface (3.50). Introducing (3.56) relation in the damage surface $\phi_1 = 0$, we have

$$\phi_1 = 0 \implies T_1 = f_t - q(\tilde{\alpha}) = f_t \exp \left[\frac{\tilde{H}}{f_t} \tilde{\alpha} \right], \quad (3.57)$$

during continuing damage. Introducing this relation in the damage evolution equations (3.51), we obtain

$$\dot{D}_{11} = \frac{\dot{\tilde{\alpha}}}{T_1} = \frac{1}{f_t} \exp \left[-\frac{\tilde{H}}{f_t} \tilde{\alpha} \right] \dot{\tilde{\alpha}}, \quad (3.58)$$

which leads, after integration,

$$\tilde{D}_{11} = \frac{1}{\tilde{H}} \left(1 - \exp \left[-\frac{\tilde{H}}{f_t} \tilde{\alpha} \right] \right) = \frac{1}{\tilde{H}} \left(1 - \frac{f_t}{T_1} \right), \quad (3.59)$$

for a continuing damage state. The combination of this last expression with the relation

$$\xi_1 = \tilde{D}_{11} T_1, \quad (3.60)$$

obtained from (3.24) and the vanishing of the cross terms \tilde{D}_{ij} ($i \neq j$), leads to

$$T_1 = f_t + \tilde{H} \xi_1, \quad (3.61)$$

a linear relation between the normal component of the traction and the crack opening displacement during loading. Finally, we also have the relation

$$\xi_1 = -\frac{f_t}{\tilde{H}} \left(1 - \exp \left[\frac{\tilde{H}}{f_t} \tilde{\alpha} \right] \right), \quad (3.62)$$

after combining (3.57) and (3.61), so $\xi_1 \in [0, -f_t/\tilde{H}]$. We consider $T_1 = 0$ for $\xi_1 \geq -f_t/\tilde{H}$.

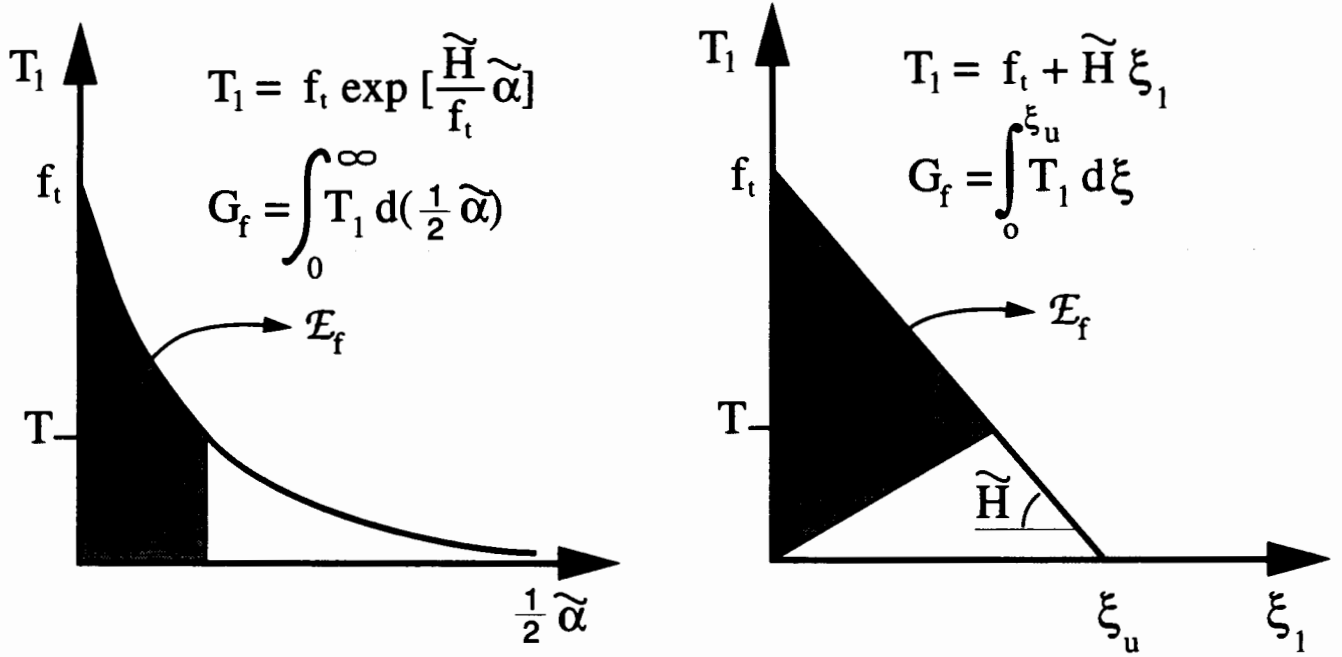


FIGURE 3.2. Equivalency of the energy released for a softening law in terms of the internal variable $\tilde{\alpha}$ or the crack opening displacement ξ_1 .

The energy release rate $\dot{\mathcal{E}}_f$ is defined as

$$\dot{\mathcal{E}}_f := \mathcal{D}_\mu + \dot{\mathcal{H}}, \quad (3.63)$$

that is, as the energy dissipation rate plus the energy rate of the (artificial) softening potential \mathcal{H} defining the cohesive opening crack. Combining (3.32) and (3.39), we conclude that

$$\dot{\mathcal{E}}_f = \left(\tilde{\mathcal{D}}_\mu - q \dot{\tilde{\alpha}} \right) \delta_{\Gamma_x} = \underbrace{\frac{1}{2} \tilde{\mathcal{D}}_{ij} T_i T_j}_{:= \dot{\tilde{\mathcal{E}}}_f} \delta_{\Gamma_x}, \quad (3.64)$$

showing the localized character of the energy released. Using the damage evolution equations (3.51), we can write this last expression as

$$\dot{\tilde{\mathcal{E}}}_f = \frac{1}{2} T_1 \dot{\tilde{\alpha}} \quad \text{in } \Gamma_x, \quad (3.65)$$

thus leading to the released energy \mathcal{E}_f in Γ_x given by

$$\tilde{\mathcal{E}}_f = \int_0^{\tilde{\alpha}_f} T_1(\tilde{\alpha}) d\left(\frac{1}{2} \tilde{\alpha}\right), \quad (3.66)$$

for a final value $\tilde{\alpha}_f$, that is, the area below the curve T_1 vs. $\tilde{\alpha}/2$. In terms of the COD ξ_1 , the energy released rate $\dot{\tilde{\mathcal{E}}}_f$ is given by

$$\dot{\tilde{\mathcal{E}}}_f = \frac{1}{2} \dot{\tilde{D}}_{11} T_1 T_1 = T_1 \dot{\xi}_1 - \frac{d}{dt} \left(\frac{1}{2} T_1 \xi_1 \right), \quad (3.67)$$

after using the relation $\xi_1 = D_{11} T_1$ and some straightforward algebraic manipulations. Therefore, the energy released in Γ_x is given by

$$\tilde{\mathcal{E}}_f = \int_0^{\xi_{1f}} \hat{T}_1(\xi_1) d\xi_1 - \frac{1}{2} T_1 \xi_1, \quad (3.68)$$

the area between the curve $T_1 = \hat{T}_1(\xi_1)$ and the degraded unloading path. Expressions (3.66) and (3.68) are depicted in Figure 3.2 for the example given by (3.56). The total fracture energy in Γ_x is then defined by

$$G_f = \int_0^{\infty} T_1(\tilde{\alpha}) d\left(\frac{1}{2}\tilde{\alpha}\right), \quad (3.69)$$

which for the case given by (3.61) reduces to the broadly used expression

$$G_f = -\frac{f_t^2}{2\tilde{H}} \quad (\tilde{H} < 0), \quad (3.70)$$

defining the linear softening modulus \tilde{H} in terms of the tensile strength f_t and fracture energy G_f .

The general case not considering the particular law (3.56) in the context of a single Mode I surface is given by the relations

$$\left. \begin{aligned} T_1 &= \hat{T}_1(\xi_1) && \text{in loading (opening crack),} \\ T_1 &= \frac{\xi_1}{\tilde{D}_{11}} && \text{in unloading (closing crack),} \end{aligned} \right\} \quad (3.71)$$

for a given scalar function $\hat{T}_1(\cdot)$, and where

$$\tilde{D}_{11} = \frac{\xi_{1,max}}{\hat{T}_1(\xi_{1,max})}, \quad (3.72)$$

in terms of the maximum crack opening displacement $\xi_{1,max} = \max\{\xi_1\}$. Relations (3.71) and (3.72) are depicted in Figure 3.3, and can be obtained directly from experiments (see REINHARDT [1984]). Full closing of the crack is obtained by imposing

$$\xi_1 \geq 0, \quad (3.73)$$

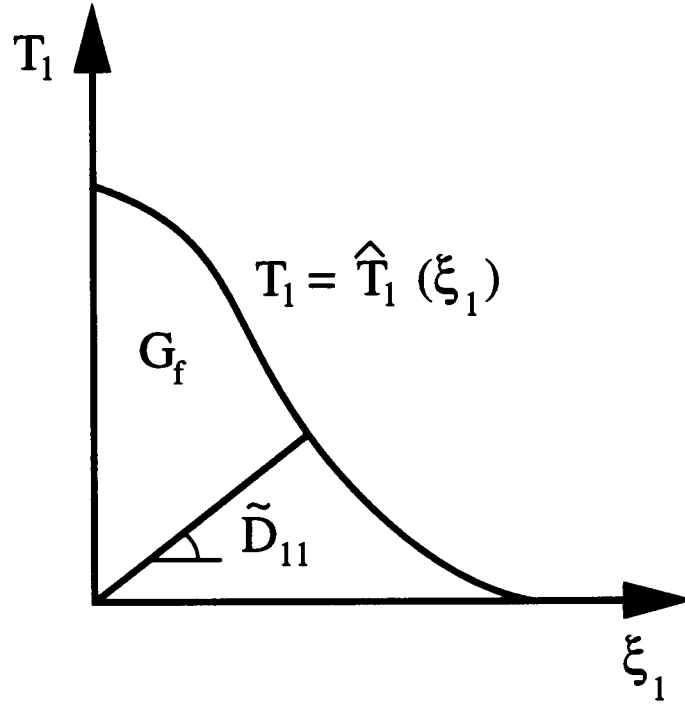


FIGURE 3.3. A softening law stress/displacement relation, with damaged unloading, characterizes the localized dissipative mechanism incorporated naturally in the model as obtained experimentally.

with

$$\tilde{D}_{11} = 0 \text{ for } \xi_1 = 0. \quad (3.74)$$

We also set $\tilde{D}_s = 0$ in this case.

For later use, we introduce the localized tangent moduli

$$\dot{T} = \tilde{C} \dot{\xi}, \quad (3.75)$$

with

$$\tilde{C} = \begin{bmatrix} \hat{T}'_1(\xi_1) & 0 \\ 0 & \tilde{D}_s^{-1} \end{bmatrix}, \quad (3.76)$$

for an opening crack (i.e., $\xi_1 = \xi_{1,max}$ and $\dot{\xi}_1 \geq 0$), and

$$\tilde{C} = \begin{bmatrix} \tilde{D}_{11}^{-1} & 0 \\ 0 & \tilde{D}_s^{-1} \end{bmatrix}, \quad (3.77)$$

for a closing crack (i.e., $0 \leq \xi_1 < \xi_{1,max}$, or $\xi_1 = \xi_{1,max}$ and $\dot{\xi}_1 < 0$).

The developments in this section have identified the formulation of constitutive model exhibiting the localized effects associated to the cracks in the material. The consideration

of the formalism of strong discontinuities allowed the introduction of these mechanisms *without the need of a length parameter defining locally a volume of damaged material*. Still, the above developments occur in the local neighborhood Ω_x . It is the goal of the following section to connect the problem posed in this neighborhood to the large-scale problem in the solid Ω , as described in Section 2. It is this connecting procedure that identifies the length scales typical of localization problems.

4. The Enhanced Strain Formulation: A Bridge of the Scales

So far, we have introduced the large-scale problem in Section 2 in terms of the smooth displacement field \mathbf{u} and the stress field $\boldsymbol{\sigma}$. Section 3 developed an anisotropic damage model locally in the neighborhood Ω_x , defining these stresses $\boldsymbol{\sigma}$ in terms of the small scale strains $\boldsymbol{\varepsilon}_\mu$ and internal variables. The large-scale strains $\boldsymbol{\varepsilon}(\mathbf{u})$ defined by (2.5) are unrelated to the unresolved strains $\boldsymbol{\varepsilon}_{unres}$ defined by (3.12) in the local neighborhood $\Omega_x \subset \Omega$. It is the goal of this section to build this relation. To that purpose, we propose next a formalism that effectively links the large-scale problem with the local model developed in the previous section. We propose in this section a “bridge of of the scales” through the formalism of the so-called enhanced strain formulation.

The enhanced strain formulation was first proposed in SIMO & RIFAI [1990] as a methodology to develop improved finite elements. The main idea is to avoid the deficiencies of standard displacement-based finite elements by adding to the strain field (enhancing) the appropriate interpolation functions that will improve the numerical performance of the finite element. The governing equations are derived from a three-field variational formulation, leading to the orthogonality between the enhanced part of the strains and the stresses. In the limit, as the finite element mesh is refined, the solution converges to the continuum solution, with the enhanced part of the strains converging to zero. The exact solution, in terms of the nodal displacement interpolating the continuum displacement field, is obtained in the limit. See the analysis presented in REDDY & SIMO [1995].

The situation in the present context is entirely different. We observe that the setting defined by the large-scale problem, as presented in Section 2, is not complete enough to define entirely the response of the solid. After the developments of Section 3.1, we can see that the unresolved part of the strain, as defined in (3.9), is completely missing in the large-scale problem (2.7). Alternatively, we can think of (3.9) as defining an “enhancement” of the large-scale strains $\boldsymbol{\varepsilon}(\mathbf{u})$ through the unresolved strains. Given the developments of Section 3, this enhancement is defined locally in the neighborhood Ω_x . In this context, we must build a “bridge” (a link) between the large-scale problem of Section 2 and the equations of the constitutive model in Ω_x in terms of the unresolved strains (depending on the displacement jumps $\boldsymbol{\xi}$) and the large-scale displacement \mathbf{u} .

We observe that the philosophy and final goal of the proposed methodology is different

than the original proposal in SIMO & RIFAI [1990]. In the limit, we want to resolve the localized dissipative effects arising from the cracking of the material, and not to obtain vanishing enhanced strains. We maintain, however, the name “enhanced strain formulation” since it emphasizes the fact that the whole approach is based on the unresolved strains (or enhanced part of the strains), rather than the local displacements \mathbf{u}_μ given by (3.1). Our main objective is to formulate a continuum model that captures the anisotropic localized effects observed in the material in the local continuum limit (i.e. as $measure(\Omega_x) \rightarrow 0$). By working with the unresolved strain fields (3.9) in terms of a yet undefined operator $\mathbf{G}(\boldsymbol{\xi})$ allows to model this limit problem without the need of requiring the compatibility of the local strains $\boldsymbol{\varepsilon}_\mu$ with a global displacement, as shown in this section. The advantages and freedom gained with these considerations are discussed in detail in what follows.

It is important to emphasize also that, given the developments of Section 3, the resulting model will resolve the dissipative localized mechanisms associated to the strong discontinuities. No “fine-scale length” is to be resolved. The model is to be understood as a large-scale model. Given the large-scale simulations of interest in this work, this feature adds considerably on the computational efficiency of the resulting numerical formulations.

The rest of this section is divided in two subsections. Section 4.1 develops these ideas in the continuum setting, leading to a well-defined formulation by “bridging the scales”. It is shown that equating the dissipation of the two problems, the large and small scale, leads to a well-defined set of equations. The resulting model is analyzed in Section 4.1.2. Section 4.2 develops a finite element formulation based on these considerations.

4.1. The “equi-dissipation bridge”

As the name of this section indicates, the basic idea in the proposed approach is to equate the dissipations, that is, *the energy dissipation rate observed in the large-scale problem must be the same as the energy dissipation rate due to the localized effects in the material*. As noted in the introduction, the main requirement in setting a large-scale problem as done in Section 2 is that the energy dissipation is captured objectively as formulated in the model developed in Section 3. By equating the two dissipations, we end up with a large-scale model that captures the localized dissipation objectively *by construction*. We show next that this simple and physically intuitive idea is enough to link the two problems.

The dissipation observed in the neighborhood $\Omega_x \subset \Omega$ of \mathbf{x} in the large-scale problem (2.7) is given by

$$\mathcal{D} = \int_{\Omega_x} \left[\boldsymbol{\sigma} : \boldsymbol{\varepsilon}(\dot{\mathbf{u}}) - \dot{\psi} \right] d\Omega_x, \quad (4.1)$$

where $\dot{\psi}$ corresponds again to the change of free energy of the material in Ω_x and $\dot{\mathbf{u}}$ is the rate of large-scale displacement \mathbf{u} . Comparing (4.1) with (3.26), we observe that the

difference between the dissipation rates at the two different scales due to the stress σ stems from the difference of the stress power measured with the large and small scale strain rates. Combining (4.1) and (3.11) with (3.26), we obtain

$$\begin{aligned} \mathcal{D} &= \int_{\Omega_x} [\sigma : \varepsilon(\dot{\mathbf{u}}) - \dot{\psi}] d\Omega_x \\ &= \mathcal{D}_\mu - \int_{\Omega_x} [\sigma : (\dot{\varepsilon}_\mu + \dot{\varepsilon}_{unres}) - \dot{\psi}] d\Omega_x \\ &= \mathcal{D}_\mu - \int_{\Omega_x} \sigma : \dot{\varepsilon}_{unres} d\Omega_x, \end{aligned} \quad (4.2)$$

for a variation $\dot{\varepsilon}_{unres}$ of the local unresolved strains.

Assumption: The dissipation rate defined by the stress field σ in the large scale problem is the same as the dissipation rate given by the localized model in Ω_x for any variation of the current equilibrium, that is, $\mathcal{D} = \mathcal{D}_\mu$.

Given (4.2), this assumption corresponds to the statement that the stress power on the unresolved strains should vanish

$$\boxed{\int_{\Omega_x} \sigma : \dot{\varepsilon}_{unres} d\Omega_x = 0,} \quad (4.3)$$

for all the variations $\dot{\varepsilon}_{unres}$ of the local unresolved strains. If we understand, as noted above, the unresolved strains as the strains enhancing the large-scale strains $\varepsilon(\mathbf{u})$, we recover *the orthogonality of the stress and the enhanced strain fields common to enhanced strain finite element formulations* (see SIMO & RIFAI [1990]).

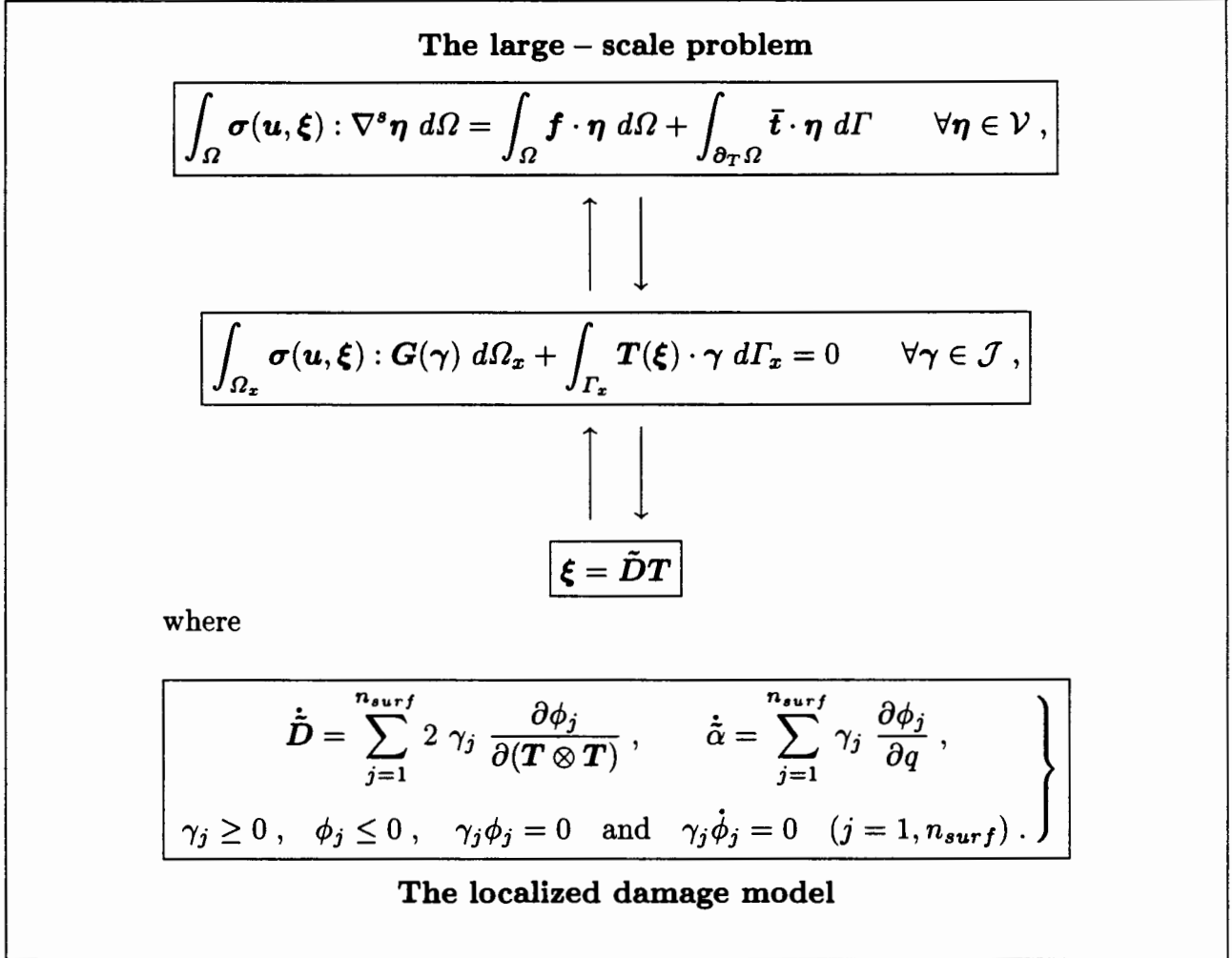
In the case of interest herein, we conclude that

$$\begin{aligned} \int_{\Omega_x} \sigma : \dot{\varepsilon}_{unres} d\Omega_x &= \int_{\Omega_x} \sigma : [\mathbf{G}(\dot{\xi}) + (\dot{\xi} \otimes \mathbf{n})^s \delta_{\Gamma_x}] d\Omega_x \\ &= \left[\int_{\Omega_x} \sigma : \mathbf{G}(\dot{\xi}) d\Omega_x + \int_{\Gamma_x} \sigma \mathbf{n} \cdot \dot{\xi} d\Gamma_x \right] \\ &= \left[\int_{\Omega_x} \sigma : \mathbf{G}(\dot{\xi}) d\Omega_x + \int_{\Gamma_x} \mathbf{T} \cdot \dot{\xi} d\Gamma_x \right], \end{aligned} \quad (4.4)$$

after using equation (3.14) for the unresolved strains and equation (3.25) defining the driving traction \mathbf{T} on Γ_x . We conclude that

$$\boxed{\int_{\Omega_x} \sigma : \mathbf{G}(\gamma) d\Omega_x + \int_{\Gamma_x} \mathbf{T} \cdot \gamma d\Gamma_x = 0 \quad \forall \gamma \in \mathcal{J}.} \quad (4.5)$$

TABLE 4.1. Summary of the governing equations. The localized damage model is introduced in the large-scale problem through the bridging equation.



This equation is to be added to the principle of virtual work (2.7) defining the the large-scale problem and the localized anisotropic model in the local neighborhood Ω_x as formulated in Section 3. The final formulation is summarized in Table 4.2. We note that the operator $\mathbf{G}(\boldsymbol{\xi})$ is still unspecified. It remains to be shown that the final set of equations determines a well-defined formulation in the sense that a solution for the unknown fields (i.e., the large-scale displacement \mathbf{u} and the crack displacement $\boldsymbol{\xi}$) can be found. We show in the next section that this is the case through a limiting procedure that recovers the local continuum framework, defining in the process the operator $\mathbf{G}(\boldsymbol{\xi})$. As shown in Section 4.1.2, equation (4.5) is enough to determine the evolution of the displacement jump $\boldsymbol{\xi}$ in terms of the large-scale displacements \mathbf{u} .

4.1.1. The consistency with the local continuum framework

An arbitrary neighborhood Ω_x , *but fixed*, has been assumed in the preceding sections. The model developed to this point exhibits then a non-local structure due to the appearance of this finite neighborhood defining the material response at the point $\mathbf{x} \in \Omega$. This situation is characteristic of non-local constitutive models, as proposed by BAZANT et al [1984], among others. As indicated in Section 1, our goal is however to formulate a constitutive model that recovers *in the limit* the local continuum framework (a *simple material* in the classical terminology introduced in TRUESDELL & NOLL [1965]), and still captures the localized dissipation as described in Section 3.

The next step is then the consideration of the limit as the measure of Ω_x tends to zero. We need to show that this limit process leads to a well-defined formulation (i.e., the bridge equation (4.5) is consistent with the weak equation (2.7) defining the large-scale problem). The analysis will lead in particular to the consistent definition of the linear operator $\mathbf{G}(\cdot)$. To this purpose, we introduce the following notation

$$A_x := \text{measure}(\Omega_x) = \int_{\Omega_x} d\Omega_x, \quad l_x := \text{measure}(\Gamma_x) = \int_{\Gamma_x} d\Gamma_x, \quad (4.6)$$

and

$$h_x := \frac{A_x}{l_x}. \quad (4.7)$$

The case of interest corresponds to $h_x \rightarrow 0$, with $A_x = O(h_x^{n_{\text{dim}}})$ and $l_x = O(h_x^{(n_{\text{dim}}-1)})$, so the neighborhood Ω_x reduces to the point \mathbf{x} in the limit. The length scale h_x is chosen as the controlling parameter in this limit process. In this context, we consider the expansions

$$\boldsymbol{\sigma}(\mathbf{y}) = \boldsymbol{\sigma}_x + O(h_x), \quad \boldsymbol{\gamma}(\mathbf{y}) = \boldsymbol{\gamma}_x + O(h_x) \quad \forall \mathbf{y} \in \Omega_x, \quad (4.8)$$

and

$$\mathbf{T}(\mathbf{y}) = \mathbf{T}_x + O(h_x) \quad \forall \mathbf{y} \in \Gamma_x, \quad (4.9)$$

where $(\cdot)_x = (\cdot)(\mathbf{x})$, that is, the value of the corresponding quantity at the fixed point $\mathbf{x} \in \Omega$. The standard notation for the “big oh” $O(\cdot)$, that is,

$$\lim_{h_x \rightarrow 0} \frac{O(h_x^k)}{h_x^k} < \infty, \quad (4.10)$$

is considered in (4.10) and (4.9).

A dimensional argument based on equation (4.5) shows that

$$\mathbf{G}(\cdot) \sim \frac{1}{h_x}, \quad (4.11)$$

after noting that the stress tensor $\boldsymbol{\sigma}$ and the traction vector \mathbf{T} are of the same order. Introducing the expansions (4.10) to (4.9), we obtain

$$\boldsymbol{\sigma}_x : \underbrace{\left[\int_{\Omega_x} \mathbf{G}(\boldsymbol{\gamma}) d\Omega_x \right]}_{O\left(\frac{A_x}{h_x}\right) = O(h_x^{n_{\text{dim}}-1})} + \mathbf{T}_x \cdot \underbrace{\boldsymbol{\gamma}_x \boldsymbol{l}_x}_{O(h_x^{(n_{\text{dim}}-1)})} + O(h_x^{n_{\text{dim}}}) = 0 \quad \forall \boldsymbol{\gamma} \in \mathcal{J}, \quad (4.12)$$

as $h_x \rightarrow 0$. Evaluation of the large-scale equation (2.12) at $\mathbf{x} \in \Omega_x$ leads to

$$\mathbf{T}_x = \boldsymbol{\sigma}_x \mathbf{n}. \quad (4.13)$$

Comparing (4.12) with (4.13), we conclude that in order for the proposed model to be consistent in the local limit $h_x \rightarrow 0$ with the local equilibrium relation (4.13) we must have

$$\int_{\Omega_x} \mathbf{G}(\boldsymbol{\gamma}) d\Omega_x = -\boldsymbol{l}_x (\boldsymbol{\gamma}_x \otimes \mathbf{n})^s + O(h_x^{n_{\text{dim}}}) \quad \forall \boldsymbol{\gamma} \in \mathcal{J}, \quad (4.14)$$

after equating the first order terms in (4.12). Dividing equation (4.14) by A_x , we obtain the equivalent relation

$$\boxed{\frac{1}{A_x} \int_{\Omega_x} \mathbf{G}(\boldsymbol{\gamma}) d\Omega_x = -\frac{1}{h_x} (\boldsymbol{\gamma}_x \otimes \mathbf{n})^s + O(1) \quad \forall \boldsymbol{\gamma} \in \mathcal{J},} \quad (4.15)$$

Therefore, the mean value of the operator $\mathbf{G}(\cdot)$ is restricted by the first order consistency condition (4.15). We conclude

$$\mathbf{G}(\boldsymbol{\gamma}) := -\frac{1}{h_x} (\boldsymbol{\gamma}_x \otimes \mathbf{n})^s + O(1) \quad \text{in } \Omega_x. \quad (4.16)$$

Higher order approximations of $\mathbf{G}(\cdot)$ can be obtained by equating higher order terms in the expansion (4.12), leading in principle to the consideration of more details of the strain field in the local neighborhood Ω_x .

Remarks 4.1.

1. As indicated in Section 4.1, the proposed methodology does not assume a-priori the compatibility between the large-scale and local displacements, leading to an incompatible unresolved strain field $\boldsymbol{\varepsilon}_{\text{unres}}$, in general. We note that stress-strain relations like (3.37), defined in terms of incompatible strains, are not uncommon. For instance, any infinitesimal elastoplastic model is based on an additive decomposition of the strain field in an elastic and plastic parts, both parts being incompatible in general. The compatibility of the unresolved strains, however, is embedded in the final proposed

formulation as the following formal argument shows. Equation (4.5) can be written formally as

$$\langle \sigma, \tilde{\mathbf{G}}(\gamma) \rangle = 0 \quad \forall \gamma \in \mathcal{J}, \quad (4.17)$$

for the operator

$$\tilde{\mathbf{G}}(\gamma) := \mathbf{G}(\gamma) + (\gamma \otimes \mathbf{n})^s \delta_{\Gamma_x}. \quad (4.18)$$

Denoting the adjoint operator $\tilde{\mathbf{G}}^*(\cdot)$, defined by the relation

$$\langle \sigma, \tilde{\mathbf{G}}(\gamma) \rangle = \langle \tilde{\mathbf{G}}^*(\sigma), \gamma \rangle \quad \forall \gamma \in \mathcal{J}, \quad (4.19)$$

we can write (4.17) as

$$\langle \tilde{\mathbf{G}}^*(\sigma), \gamma \rangle = 0 \quad \forall \gamma \in \mathcal{J}, \quad (4.20)$$

The argument presented in this section imposes the operator $\tilde{\mathbf{G}}^*(\cdot)$ to be consistent to the desired order in h_x with the local equilibrium equation (4.13). We recover then to the desired order the compatibility of the unresolvable strains defined by $\tilde{\mathbf{G}}(\cdot)$ in the sense of being defined by *duality* to the equilibrium operator. Existence and regularity analyses of elastoplastic models based on the mechanical equations written in dual form as in (4.20), with a complete discussion of the above arguments, can be found in MATTHIES et al [1979], JOHNSON [1976], JOHNSON [1978] and SUQUET [1981].

2. We note that the Taylor's expansions considered in (4.10) and (4.9) involve regular fields. In particular, we consider the (smooth) displacement jumps and not the strains. This situation is to be contrasted with the typical argument that relates traditional non-local models with higher-order models in terms of a Taylor's expansion of the total strain field, which becomes singular (unbounded), making the expansion argument questionable. See PIJAUDIER-CABOT et al [1995] for a discussion of these issues. \square

4.1.2. Analysis of the model

It remains to show that the displacement jump $\boldsymbol{\xi}$ is determined with the equation (4.5), locally in Ω_x . To this purpose, we introduce the expression (4.16) characterizing the unresolved strains in the limit of interest in the governing equation (4.5) to obtain

$$\mathbf{T}(\boldsymbol{\xi}_x) = \frac{1}{A_x} \int_{\Omega_x} \boldsymbol{\sigma} \mathbf{n} \, d\Omega_x + O(h_x) = \frac{1}{A_x} \int_{\Omega_x} \mathbf{C}^e [\boldsymbol{\varepsilon}(\mathbf{u}) + \mathbf{G}(\boldsymbol{\xi})] \mathbf{n} \, d\Omega_x + O(h_x), \quad (4.21)$$

after dividing by l_x and making use of the constitutive relation (3.37). Equation (4.21) identifies the traction vector at \mathbf{x} as the average value arising from the stress field in Ω_x , up to terms $O(h_x)$, as we would expect after the considerations in the previous section.

Rearranging the terms in (4.21) leads to the nonlinear algebraic equation in $\boldsymbol{\xi}_x \in \mathbb{R}^{n_{\text{dim}}}$

$$\frac{1}{h_x} \mathbf{Q}^e \boldsymbol{\xi}_x + \mathbf{T}(\boldsymbol{\xi}_x) = \mathbf{F}(\mathbf{u}), \quad (4.22)$$

where we have introduced the linear operator

$$\mathbf{F}(\mathbf{u}) := \frac{1}{A_x} \int_{\Omega_x} [\mathbf{n} \cdot \mathbf{C}^e \boldsymbol{\varepsilon}(\mathbf{u})] d\Omega_x + O(h_x). \quad (4.23)$$

The tensor $\mathbf{Q}^e \in \mathbb{R}^{n_{\text{dim}} \times n_{\text{dim}}}$ corresponds to the elastic acoustic tensor in the direction \mathbf{n} defined as

$$Q_{ik}^e := C_{ijkl}^e n_j n_l, \quad (4.24)$$

and is assumed, without loss of generality, positive definite. For instance, under the usual assumption of isotropic elastic response

$$C_{ijkl}^e = \lambda \delta_{ij} \delta_{kl} + \mu [\delta_{ik} \delta_{jl} + \delta_{il} \delta_{jk}], \quad (4.25)$$

for Lamé constants λ and μ , the acoustic tensor (4.24) reads

$$Q_{ik}^e = \mu \delta_{ik} + (\lambda + \mu) n_i n_k, \quad (4.26)$$

which is positive definite if $\mu > 0$ and $\lambda + 2\mu > 0$.

Consider the eigenvalue problem

$$\tilde{\mathbf{C}} \mathbf{a} = \omega \mathbf{Q}^e \mathbf{a}, \quad (4.27)$$

in the eigenvalues $\omega \in \mathbb{R}$ and eigenvectors $\mathbf{a} \in \mathbb{R}^{n_{\text{dim}}}$, where $\tilde{\mathbf{C}}$ corresponds to the localized tangent matrix defined in (3.75). Then, a solution of (4.21) in the limit of interest $h_x \rightarrow 0$ is assured by the implicit function theorem (non-zero derivative of the left-hand side of (4.21)) as long as

$$\omega_{\min} + \frac{1}{h_x} > 0, \quad (4.28)$$

where $\omega_{\min} = \min\{w_1, \dots, w_{n_{\text{dim}}}\}$. Condition (4.28) is satisfied by taking h_x sufficiently small, under the assumption of finite ω_{\min} . We conclude that the model developed in the previous sections determines the displacement jump $\boldsymbol{\xi}$ in the limit $h_x \rightarrow 0$ characterizing the local small scale fields in terms of the large-scale displacement \mathbf{u} , as indicated by the nonlinear equation (4.22). After solving this local equation, the large scale problem is completely formulated entirely in terms of the large-scale field \mathbf{u} . Constant elastic moduli \mathbf{C}^e in Ω_x have been assumed in writing (4.22). The general case is recovered by assuming the average value in the local neighborhood Ω_x .

It is also interesting to observe that given (4.22) and the boundedness of the elastic moduli and stress, we conclude that

$$\mathbf{n} \cdot \mathbf{C}^e \boldsymbol{\varepsilon}(\mathbf{u}) \sim \frac{1}{h_x} \mathbf{Q}^e \boldsymbol{\xi}_x + O(1) \quad \text{in} \quad \Omega_x, \quad (4.29)$$

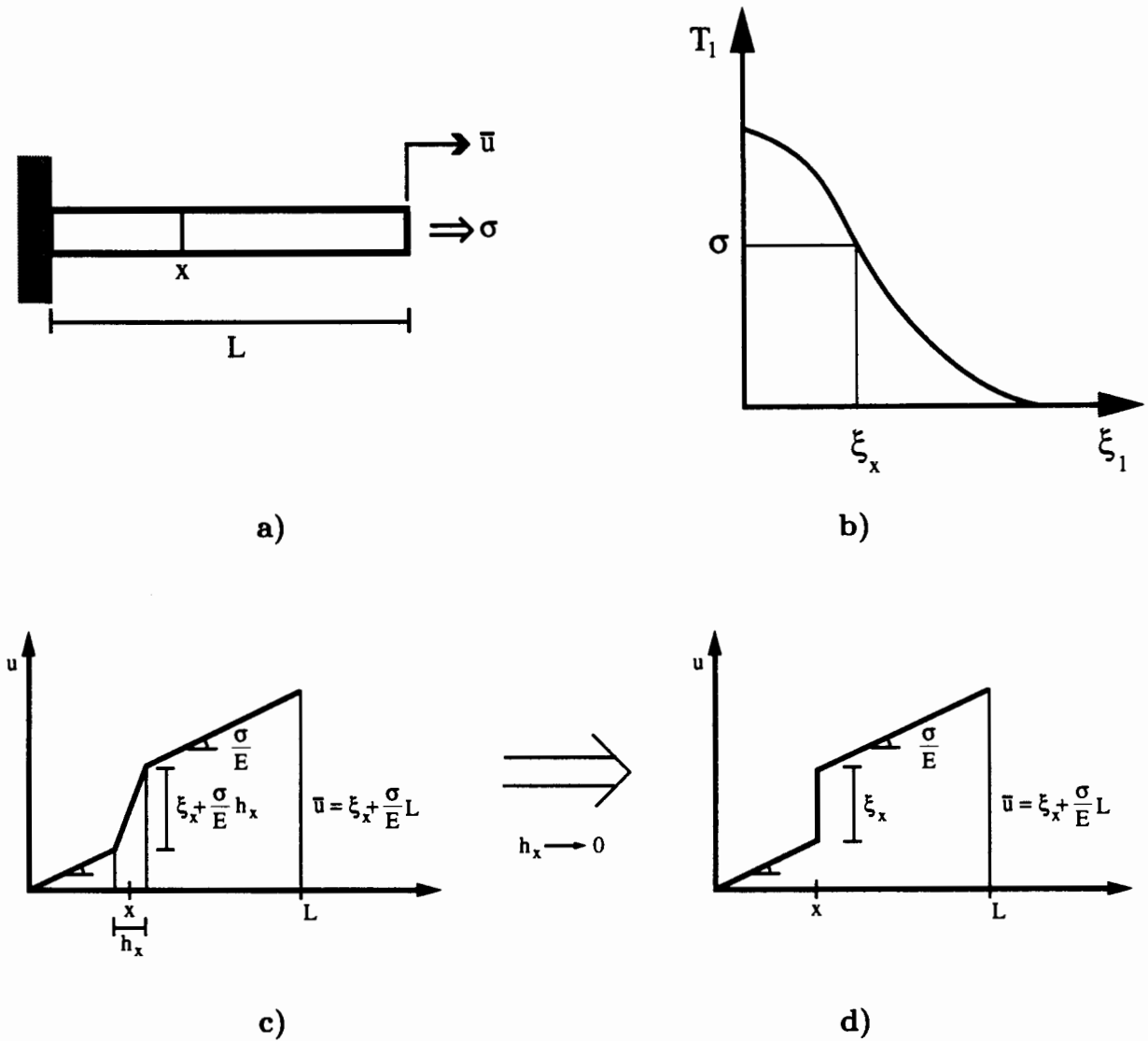


FIGURE 4.1. One dimensional cracking problem. **a)** Problem definition: bar under imposed displacement \bar{u} at the tip. **b)** Stress/displacement relation. **c)** Large-scale displacement field $u(x)$ for finite h_x and **d)** for the limit problem $h_x = 0$. In this last case, the large-scale displacement resolves the jump discontinuity associated to the crack.

identifying the singularity of the strains in the limit problem $h_x = 0$ in a set of $measure(\Omega_x) = O(h_x^{n_{dim}})$. Note that as $h_x \rightarrow 0$, the neighborhood Ω_x collapses to the material point x , with the total strain is given only by the large-scale field $\epsilon(\mathbf{u})$ near the discontinuity. Physically, the result (4.29) states that in the limit $h_x \rightarrow 0$, the strain field in the large-scale problem of interest captures the singularity introduced by the strong discontinuity, being of the order $1/h_x$ at a distance h_x from it.

In the limit problem $h_x = 0$, the large-scale fields resolve the strains associated to the

strong discontinuities at $\Gamma = \{\mathbf{x}$, where localization has been detected}. This situation is depicted in Figure 4.1 for a straight rod in $n_{\text{dim}} = 1$ with $\Omega = [0, L]$. An imposed displacement is applied at the right end whereas the left end is assumed fixed. No body forces are applied. The equilibrium equations identify then the axial stresses σ as constant. A strong discontinuity is assumed to form at \mathbf{x} (due to, say, an imperfection) when $\sigma = f_t$, so $\Gamma \equiv \mathbf{x}$. The constant stress distribution leads to a linear distribution of the displacement u outside the neighborhood $\Omega_{\mathbf{x}} = (x - h_{\mathbf{x}}/2, x + h_{\mathbf{x}}/2)$. Since both the stress σ and the jump distribution $\xi_{\mathbf{x}}$ are constant in $\Omega_{\mathbf{x}}$, the strain $\varepsilon(u)$ is constant as well in $\Omega_{\mathbf{x}}$, leading to the linear distribution of u in $\Omega_{\mathbf{x}}$. The jump $\xi_{\mathbf{x}}$ is given in terms of the applied stress by equation (4.22). As $h_{\mathbf{x}} \rightarrow 0$, we observe that the large-scale displacement field u resolves in the limit the jump singularity associated to the crack.

The above developments have identified the properties of the proposed anisotropic damage model. In particular, we conclude that the effects of the localized dissipation associated to the formation and opening of cracks in the material can be built into a large-scale model involving the desired smoothness of the unknown fields for their numerical resolution. The following section describes a finite element method based on these considerations.

4.2. Finite element implementation

The formulation developed in the previous section can be incorporated very easily in a finite element formulation in the framework of assumed enhanced strain methods as presented originally in SIMO & RIFAI [1990]. In fact, the above developments are very much inspired in the resulting numerical formulations as described in ARMERO & GARIKIPATI [1995,96] for localization problems in infinitesimal and finite strain plasticity.

Consider the discretized large-scale strains defined as

$$\varepsilon(\mathbf{u}^h) = \mathbf{B} \mathbf{d}, \quad (4.30)$$

in a typical finite element Ω_e , where \mathbf{B} denotes the standard linearized strain operator arising from a standard finite element interpolation

$$\mathbf{u}^h = \mathbf{N}^h \mathbf{d}, \quad (4.31)$$

for some interpolation functions \mathbf{N}^h and corresponding \mathbf{d} . The simulations of Section 5 consider linear triangles. Mixed or assumed strain interpolations can be incorporated easily at this stage, so \mathbf{B} refers to these general cases. See ARMERO & GARIKIPATI [1995,96] for the consideration of higher order mixed triangles in the pressure, in the context of Mises plasticity.

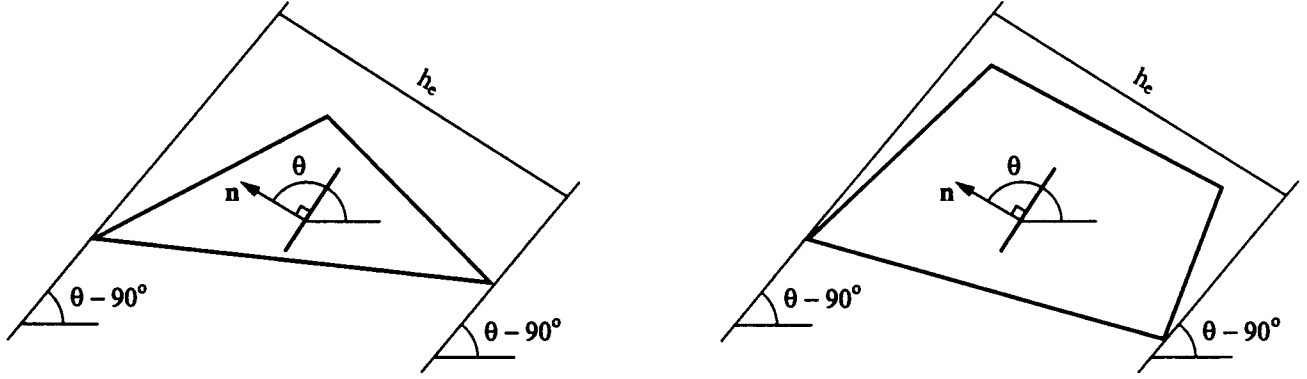


FIGURE 4.2. Determination of the length parameter h_e for triangular and quadrilateral finite elements.

The neighborhood Ω_x in the arguments above is taken to be a finite element Ω_e where localization has been detected ($\sigma_{max} = f_t$ at some point of the element). The interpolated total strain ϵ_μ^h is then given following the developments of Section 4.1 as

$$\epsilon_\mu^h = \epsilon(\mathbf{u}^h) + \epsilon_{unres}^h, \quad (4.32)$$

with the unresolved strain (or, equivalently, in this context *the enhanced part*) is given by (3.14) as

$$\epsilon_{unres}^h = \mathbf{G}_e \xi_e^h + \tilde{\mathbf{P}}_e \xi_e^h \delta_{\Gamma_e}, \quad (4.33)$$

where $\xi_e \in \mathbb{R}^{n_{dim}}$ denotes a set of n_{dim} unknown parameters and, for a plane problem,

$$\tilde{\mathbf{P}}_e = \begin{bmatrix} \cos^2 \vartheta & -\cos \vartheta \sin \vartheta \\ \sin^2 \vartheta & \cos \vartheta \sin \vartheta \\ \sin 2\vartheta & \cos 2\vartheta \end{bmatrix}, \quad (4.34)$$

in the standard vector notation for the strain field, with ϑ being the angle between the normal to the crack and the x_1 cartesian direction. Constant enhanced parameters $\xi_e^h \in \mathbb{R}^{n_{dim}}$ are introduced in a localized element, approximating the corresponding crack displacements ξ as employed in the previous sections are considered. Higher order interpolations can be accommodated following the remarks leading to (4.16).

The strain operator \mathbf{G}_e in (4.33) is defined after (4.16) as

$$\mathbf{G}_e = -\frac{1}{h_e} \tilde{\mathbf{P}}_e \quad \text{in } \Omega_e, \quad (4.35)$$

with $\tilde{\mathbf{P}}_e$ given by (4.34), and vanishes outside Ω_e . The element parameter h_e is defined in (4.7) as the ratio of the $A_e = \text{measure}(\Omega_e)$ and of the surface $l_e = \text{measure}(\Gamma_e)$ of the considered neighborhood (Ω_e in this case). Since the definition of Γ_e in $n_{dim} > 1$ is inherently arbitrary (an extension of the crack at \mathbf{x}), the definition of h_e is also arbitrary,

except for the consistency condition $h_e \rightarrow 0$ as the finite element mesh is refined (i.e., a measure of the element size). In the 1D case $n_{\text{dim}} = 1$, we have $l_e = 1$ and $A_e = h_e$ (see Figure 5.1), so in contrast h_e is well-defined. As shown in the numerical simulation presented in Section 5.1, the exact solution depicted in Figure 5.1 is obtained for the proposed finite element formulation in this one-dimensional case. With this background, we consider the length parameter h_e as defined in Figure 4.2, for triangular and quadrilateral finite elements and the given orientation ϑ of the crack. With this definition the exact solution is obtained again for the simulation of a 1D rod employing an aligned mesh, as presented in Section 5.1.

We note that for the general case of a discontinuity Γ_e not aligned with any side of the triangular element the strain given by (4.33) is not the gradient of a compatible displacement field (that is, vanishing at the nodes). Still, the formulation developed in the previous section allows the proposed interpolations, without the need of the pointwise satisfaction of the kinematic compatibility constraint. The added freedom is clearly to the advantage of formulating efficient numerical formulations. The compatibility constraints are effectively imposed in the limit as noted in Remark 4.1.1. We refer to ARMERO & GARIKIPATI [1995,96] for finite element formulations in the framework of elastoplasticity based on discrete unresolved strains (4.35) obtained as the gradient of discontinuous interpolation functions on a triangle, leading to unsymmetric formulations.

The proposed formulation falls in the class of assumed strain methods as proposed originally by SIMO & RIFAI [1990]. The unresolved strains corresponds to the *enhanced part* of the strain, that is,

$$\boldsymbol{\varepsilon}_\mu^h = \underbrace{\mathbf{B}d}_{\text{conforming}} + \underbrace{\tilde{\mathbf{G}}_e \boldsymbol{\xi}_e^h}_{\text{enhanced}}, \quad (4.36)$$

for the enhanced strain operator $\tilde{\mathbf{G}}_e$ defined by

$$\tilde{\mathbf{G}}_e := -\frac{1}{h_e} \tilde{\mathbf{P}}_e + \tilde{\mathbf{P}}_e \delta_{\Gamma_e}. \quad (4.37)$$

We note that the consistency condition identified in SIMO & RIFAI [1990] for the satisfaction of the patch test, namely

$$0 = \int_{\Omega_e} \tilde{\mathbf{G}}_e d\Omega = \tilde{\mathbf{P}}_e \left[-\frac{l_e}{A_e} A_e + \underbrace{\int_{\Omega_e} \delta_{\Gamma_x} d\Omega}_{= \int_{\Gamma_e} d\Gamma =: l_e} \right], \quad (4.38)$$

is satisfied, a clear consequence of the developments of Section 4.1.1.

The finite element formulation is based on the discrete counterpart of the weak equa-

tion (2.7) and the local nonlinear equation (4.22)

$$\left. \begin{aligned} \mathbf{R} &:= \mathbf{f}_{ext} - \mathbf{A} \int_{\Omega_e} \mathbf{B}^T \boldsymbol{\sigma} \, d\Omega = 0 \\ \mathbf{s}_e &:= \mathbf{F}_e \mathbf{d} - \left[\frac{1}{h_e} \mathbf{Q}^e \boldsymbol{\xi}_e^h + \mathbf{T}(\boldsymbol{\xi}_e^h) \right] = 0 \quad \text{in } \Omega_e \end{aligned} \right\}, \quad (4.39)$$

where

$$\mathbf{F}_e(\mathbf{d}) := \frac{1}{A_e} \int_{\Omega_e} [\mathbf{n} \cdot \mathbf{C}^e \mathbf{B}] \, d\Omega_e. \quad (4.40)$$

after (4.23), and the stress $\boldsymbol{\sigma}$ is given by

$$\boldsymbol{\sigma} = \mathbf{C}^e [\mathbf{B} \mathbf{d} + \mathbf{G}_e \boldsymbol{\xi}_e^h]. \quad (4.41)$$

We note the independence of the enhanced parameters from element to element, consistent with the local character of the decomposition (3.7). As a practical consequence, this leads to the efficient implementation of the proposed formulation through the static condensation of the enhanced parameters as described below.

The system of equations (4.39), in the nodal displacements \mathbf{d} and local enhanced parameters $\boldsymbol{\xi}_e^h$ is nonlinear due to the nonlinearity of the cohesive softening law (4.39)₂. This system is solved using a standard Newton-Raphson technique involving the consistent linearization of the equations. The different steps for a typical time increment, say, $[t_n, t_{n+1}]$ are summarized in Table 4.4. In a first step, the new enhanced parameters $\boldsymbol{\xi}_{e, n+1}^{h(k)}$ at a given iteration (k) are obtained in terms of the current values of the nodal displacements $\mathbf{d}_{n+1}^{(k)}$. The global residual and stiffness matrix is then assembled after the static condensation of these parameters, leading to the algebraic system of equations (4.45) in terms of the nodal displacements only. An alternative implementation involving of the local Newton iteration (4.42) coupled with the global Newton-Raphson scheme (4.45) has been described in ARMERO [1997]; see this reference for details. The final set of equations (4.45) in the nodal displacements \mathbf{d} corresponds to the large-scale problem described in Section 2 incorporating the dissipation of the small scale effects *objectively by construction*, as it was the original goal of the proposed formulation of a large-scale model incorporating the localized dissipative mechanisms of the material.

Remark 4.2. Traditional smeared crack approaches (see e.g. BAZANT & OH [1983], ROTS et al [1985]) are effectively recovered with the proposed formulation by considering the following interpolations of the enhanced strains

$$\boldsymbol{\varepsilon}_{unres}^h \sum_{l=1}^{n_{int}} \left[\mathbf{G}_l(\boldsymbol{\xi}_l^h) N_l(\mathbf{x}) + \bar{\mathbf{P}}_l \boldsymbol{\xi}_l \delta_{\Gamma_l} \right], \quad (4.46)$$

TABLE 4.3. Integration algorithm for a time increment $[t_n, t_{n+1}]$.

Given $\xi_{e_n}^h$ (the converged value at t_n), $\xi_{1,max_n}^h = \max_{i=1,n}\{\xi_{1,i}^h\} \geq 0$ and $\tilde{D}_{11,n}$, and given a current iteration $\mathbf{d}_{n+1}^{(k)}$ of the nodal displacements (n being the index for the current time increment, and k the index for the current iteration), then

1. Update the enhanced parameters $\xi_{e_{n+1}}^{h(k)}$ by solving (4.39)₂ with fixed $\mathbf{d}_{n+1}^{(k)}$, using Newton's method

$$\left. \begin{aligned}
 & l = 0 \\
 & \text{DO WHILE } e.g. \|\mathbf{s}_e(\xi_{e_{n+1}}^{h(k,l)})\| \leq \text{TOL} \\
 & \quad \mathbf{H}_{e_{n+1}}^{(k,l)} := \frac{1}{h_e} \mathbf{Q}^e + \tilde{\mathbf{C}}(\xi_{1,max_n}^h) \\
 & \quad \xi_{e_{n+1}}^{h(k,l+1)} = \xi_{e_{n+1}}^{h(k,l)} + [\mathbf{H}_{e_{n+1}}^{(k,l)}]^{-1} \mathbf{s}_e(\xi_{e_{n+1}}^{h(k,l)}) \\
 & \quad l \leftarrow l + 1 \\
 & \text{END DO}
 \end{aligned} \right\} \quad (4.42)$$

starting with the initial estimate given by the converged value $\xi_{e_{n+1}}^{h(k,0)} = \xi_{e_n}^h$ at the previous time step. The tangent $\tilde{\mathbf{C}}(\cdot)$ in (4.42) is given by (3.76) for an opening crack ($\xi_{e_{1,n+1}}^{h(k,l)} \geq \xi_{1,max_n}^h$) or (3.77) for a closing crack ($0 \leq \xi_{e_{1,n+1}}^{h(k,l)} \leq \xi_{1,max_n}^h$). If a closed crack is detected ($\xi_{e_{1,n+1}}^{h(k,l)} < 0$), then we set $\xi_{e_{n+1}}^{h(k)} = 0$.

2. Compute the statically condensed residual

$$\mathbf{R}_{n+1}^{*(k)} := \mathbf{f}_{ext} - \mathbf{A} \left\{ \int_{\Omega_e} \mathbf{B}^T \mathbf{C}^e [\mathbf{B} \mathbf{d}_{n+1}^{(k)} + \mathbf{G}_e \xi_{e_{n+1}}^{h(k)}] d\Omega - \mathbf{L}_e [\mathbf{H}_{e_{n+1}}^{(k)}]^{-1} \mathbf{s}_e(\xi_{e_{n+1}}^{h(k)}) \right\} \quad (4.43)$$

where $\mathbf{L}_e := \int_{\Omega_e} \mathbf{B}^T \mathbf{C}^e \mathbf{G}_e d\Omega$ for the elastic tangent \mathbf{C}^e given by (4.25).

3. Assemble the statically condensed stiffness matrix

$$\mathbf{K}_{n+1}^{*(k)} := \mathbf{A} \left\{ \int_{\Omega_e} \mathbf{B}^T \mathbf{C}^e \mathbf{B} d\Omega - \mathbf{L}_e [\mathbf{H}_{e_{n+1}}^{(k)}]^{-1} \mathbf{L}_e^T \right\}, \quad (4.44)$$

4. Solve and update nodal displacements

$$\mathbf{K}_{n+1}^{*(k)} \Delta \mathbf{d}_{n+1}^{k+1} = \mathbf{R}_{n+1}^{*(k)} \quad \text{with} \quad \mathbf{d}_{n+1}^{(k+1)} = \mathbf{d}_{n+1}^{(k)} + \Delta \mathbf{d}_{n+1}^{(k+1)}. \quad (4.45)$$

with

$$\mathbf{G}_l(\boldsymbol{\xi}_l) := -\frac{1}{h_l} (\boldsymbol{\xi}_l^h \otimes \mathbf{n})^s = -\frac{1}{h_l} \tilde{\mathbf{P}}_l \boldsymbol{\xi}_l^h, \quad (4.47)$$

for each quadrature point $l = 1, n_{int}$. In (4.46), we made use of the shape functions $N_l(\mathbf{x})$ based on the quadrature points \mathbf{x}_l , $l = 1, n_{int}$ (i.e., $N_l(\mathbf{x}_j) = \delta_{lj}$, $j = 1, n_{int}$). The matrix $\tilde{\mathbf{P}}_l$ and length parameter h_l are defined as in (4.34) and Figure 4.2, respectively, for a given crack direction ϑ_l at quadrature point $l = 1, n_{int}$. With this setting, the contributions of the enhanced strains for each quadrature point decouple, leading to the counterpart of equation (4.42)

$$\mathbf{s}_l := \tilde{\mathbf{P}}_l^T \mathbf{C}^e \mathbf{B}_l \mathbf{d} - \left[\frac{1}{h_l} \mathbf{Q}_l^e \boldsymbol{\xi}_l^h + \mathbf{T}(\boldsymbol{\xi}_l^h) \right] = 0 \quad l = 1, n_{int}, \quad (4.48)$$

solved locally as in (4.42) at each quadrature point $l = 1, n_{int}$. The resulting statically condensed residual is given

$$\begin{aligned} \mathbf{R}_{n+1}^{*(k)} := \mathbf{f}_{ext} - \mathbf{A} \left\{ \sum_{e=1}^{n_{elem}} \mathbf{B}_l^T \mathbf{C}^e \left[\mathbf{B}_l \mathbf{d}_{n+1}^{(k)} \right. \right. \\ \left. \left. - \frac{1}{h_l} \tilde{\mathbf{P}}_l \left(\boldsymbol{\xi}_{l\ n+1}^{h(k)} + \left[\mathbf{H}_{l\ n+1}^{(k)} \right]^{-1} \mathbf{s}_{l\ n+1}^{(k)} \right) \right] \mathbf{A}_l \right\}, \end{aligned} \quad (4.49)$$

and the statically condensed stiffness matrix

$$\mathbf{K}_{n+1}^{*(k)} := \mathbf{A} \left\{ \sum_{l=1}^{n_{int}} \mathbf{B}_l^T \left[\mathbf{C}^e - \frac{1}{h_l} \mathbf{C}^e \tilde{\mathbf{P}}_l \left[\mathbf{H}_{l\ n+1}^{(k)} \right]^{-1} \tilde{\mathbf{P}}_l^T \mathbf{C}^e \right] \mathbf{B}_l \mathbf{A}_l \right\}. \quad (4.50)$$

where \mathbf{A}_l is the measure associated to the quadrature point $l = 1, n_{int}$ after using the discrete quadrature rule ($\mathbf{A}_l = w_l \mathbf{j}_l$ for a weight w_l and Jacobian of the isoparametric map \mathbf{j}_l). Relations of the form (4.49) and (4.50) are common in smeared crack models (see e.g. ROTS et al [1985]), but with an important difference. As noted in Remark 3.2.1, the shear response in the proposed formulation is given by a shear stress/slip displacement relation, as given by the localized shear compliance $\tilde{\mathbf{D}}_s$, in (3.53), rather than a stress/strain relation. The consideration of constant degraded shear stress/displacement laws was presented in ARMERO [1997] in this context. In a more general setting, the localized stress/displacement law $\mathbf{T}_l = \mathbf{T}(\boldsymbol{\xi}_l^h)$ is defined by $\boldsymbol{\xi}_l^h = \tilde{\mathbf{D}}_l \mathbf{T}_l$ with the crack compliances $\tilde{\mathbf{D}}$ being degraded continuously by the evolution equations (3.47), leading to a general multi-surface *localized anisotropic damage model*. \square

a)



b)

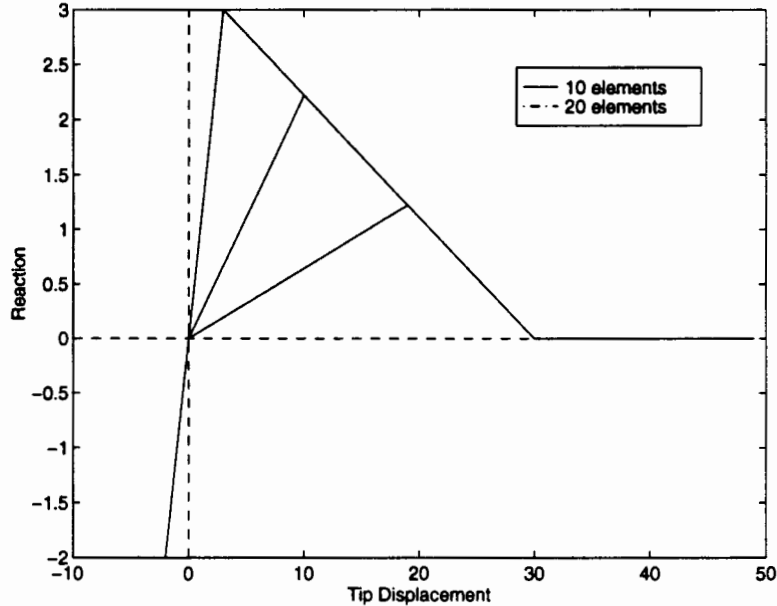


FIGURE 5.1. Rod under uniaxial stress. **a)** Solution at a tip displacement of 30 for the 20 element mesh. All the displacement is localized in the finite elements with active enhanced modes (in gray). **b)** The load-displacement curves for two different meshes overlap the exact solution.

5. Representative Numerical Simulations

We present in this section two representative numerical simulations that illustrate the performance of the finite element formulation described in the previous section. The solution to the tensile test of a straight rod is considered in Section 5.1. Section 5.2 presents the solution to the three-point bend test of a beam in plane stress conditions. The localized anisotropic damage model involving only the mode I surface (3.50) is considered.

5.1. Tensile test of a straight rod

Figure 5.1 shows the results obtained in the uniaxial test of a straight rod. The total length of the rod is 10. and it has an unit cross section area. The values of Young modulus $E = 10$, Poisson's ratio $\nu = 0$, tensile strength $f_t = 3$, and softening modulus $\tilde{H} = 0.1$ are assumed. A linear softening $\mathbf{T} = \mathbf{T}(\xi)$ law is employed. We consider two discretizations, involving 10 and 20 linear triangles, respectively. Figure 5.1 depicts the discretization with 20 elements in an aligned mesh. To trigger the localization of the cracking an imperfection of 0.1% in the tensile strength is assumed in the first two elements.

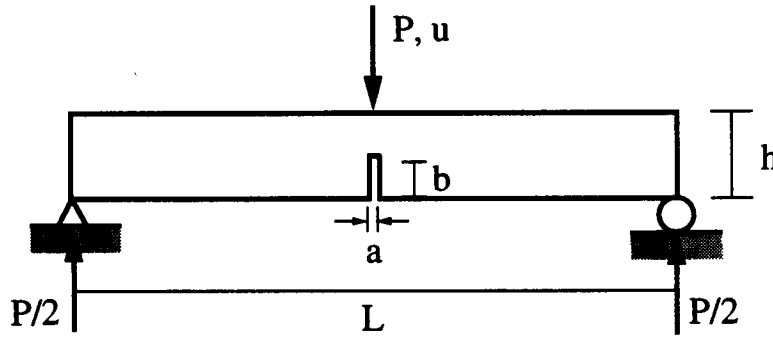


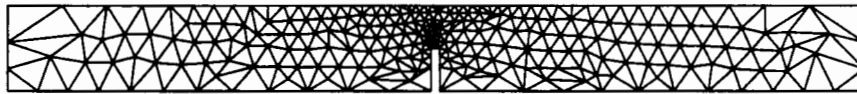
FIGURE 5.2. Three-point bend test. Problem definition: $L = 200 \text{ mm}$, $h = 20 \text{ mm}$, $a = 2 \text{ mm}$, and $b = 10 \text{ mm}$. Imposed downward displacement u and measured P .

The solution obtained with the 20 element mesh is depicted in Figure 5.1.a, showing all the tip displacement accumulated in the two elements that soften. All the numerical simulations are run with imposed displacements at the tip. Figure 5.1.b depicts the computed load displacement curves for the two meshes. Both overlap the exact solution, as depicted in Figure 4.1, showing the mesh-size independence of the numerical solution. We note that some formulations proposed in the literature do not obtain the exact solution in this simple 1D setting (see SLUYS [1997]), due to the different definition of the crack length used in the finite element strain fields. The solution depicted in Figures 5.1 considers also the unloading, closing of the crack, and reloading paths. Exact solutions are again obtained with the finite element formulation presented herein.

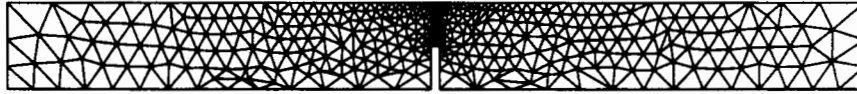
5.2. Three-point bend test

This second example considers the three-point bend test of a notched rectangular beam. Figure 5.2 depicts the geometry of the specimen, a $200 \times 20 \times 1 \text{ mm}^3$ plain concrete beam with $2 \times 10 \text{ mm}^2$ notch, as presented in PETERSSON [1984]. Plane stress conditions are assumed through the thickness. The material parameters are given by Young modulus $E = 3 \cdot 10^4 \text{ N/mm}^2$, Poisson's ratio $\nu = 0.2$, tensile strength $f_t = 3.33 \text{ N/mm}^2$, fracture energy $G_f = 0.124 \text{ N/mm}$ (hence, a localized linear softening modulus $\tilde{H} = -f_t^2/(2G_f)$ is considered), and a degraded crack shear compliance of $\tilde{D}_s^{crack} = 8 \cdot 10^{-2} \text{ mm/N}$.

The numerical simulations are run with an imposed downward displacement at the top middle-span. Unstructured meshes are considered as shown in Figure 5.3 with a total of 442 and 654, respectively. Figure 5.4.a depicts the solution obtained with the coarse mesh (a magnification of 100 is considered). Figure 5.4.a shows the details of the solution in the notch, showing the accumulation of the strains in the elements with active localized enhanced modes (in gray). Figure 5.4.b includes the load/displacement curves obtained for the different unstructured meshes. The difference observed between the solutions obtained with different meshes are a consequence of the different level of approximation for each mesh rather than the lack of objectivity of the solution.

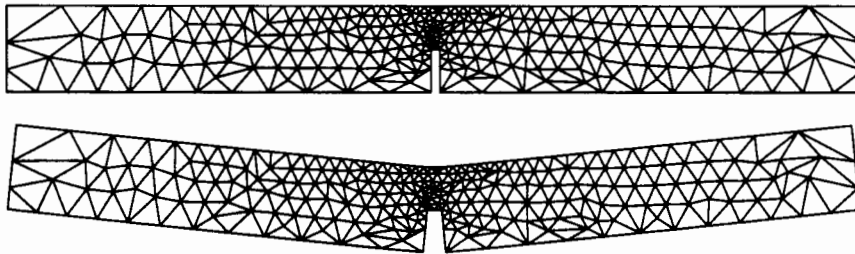


442 element mesh

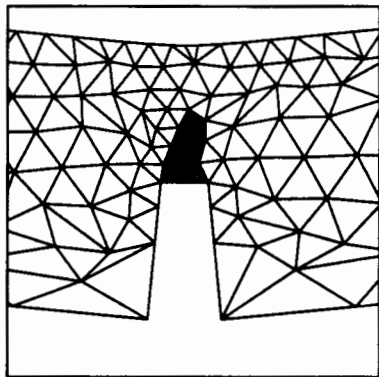


654 element mesh

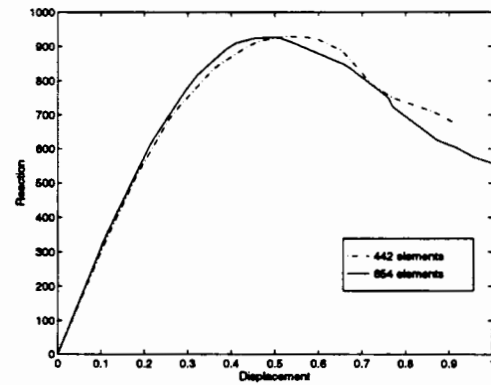
FIGURE 5.3. Three-point bend test. Assumed spatial discretizations: 442 and 654 element meshes.



a)



b)



c)

FIGURE 5.4. Three-point bend test. **a)** Initial and deformed configurations at an imposed displacement of 0.1 (442 element mesh, magnification 100). **b)** Detail showing the elements with active enhanced modes. **c)** Load-displacement curves for two different discretizations.

6. Conclusions

After the developments presented in the preceding sections, we can draw the following conclusions:

1. The consideration of strong discontinuities (through a formalism based on distribution theory) allows the formulation of anisotropic damage models that incorporate the localized dissipation characteristic of brittle solids under tension (cracking). The resulting model determines the local response of the solid.
2. The consideration of the principle of maximum damage dissipation determines the evolution equations of the *localized* internal variables describing the damage of the material. In particular, a precise definition of the evolution of the compliance added by the presence of a crack can be obtained through the proposed methodology.
3. The resulting local anisotropic damage model incorporates naturally the stress/crack-displacements relations obtained in typical experiments. In this way, the local model incorporates the localized dissipative mechanism associated to the cracks in the material without the need of smoothing or smearing the associated discontinuous displacement and corresponding singular strains.
4. The local singular strain fields characterizing the damage of the material can be efficiently incorporated in a large scale problem in terms of smooth fields through the consideration of the enhanced strain method. The proposed methodology accomplishes this "bridge between the scales" by matching the dissipation observed in each problem. Since, as indicated in Item 3, the localized damage model captures the dissipation objectively, the resulting large-scale problem will dissipate the energy *objectively by construction* following the proposed methodology.
5. The resulting formulation is shown to be well-defined, with the local singular fields being determined by the assumed smooth fields in the large scales. Furthermore, the limit as the small scales vanish is shown to be consistent with the local continuum framework. The proposed model is understood as a large-scale model, incorporating efficiently the dissipative mechanisms observed in the large-scale applications of interest, without the costly need to resolve fine length scales of the local response of the material.
6. The constitutive model developed with this procedure can be naturally incorporated in a finite element formulation. The resulting method requires a local update of the localized internal variables (crack displacements) at the element level, leading to an efficient implementation in terms of the nodal displacements only.
7. Traditional numerical treatments of the problem based on the so-called smeared crack approach can be effectively obtained through the proposed methodology. The shear response of the crack involves, however, a natural stress/displacement relations, rather

than a smeared relation. This link has identified then the connection of these commonly used smeared models with anisotropic damage models that describe the localized damage based on sound thermodynamical principles.

8. This link adds generality to traditional smeared crack models through extensions easily incorporated to the formulation of anisotropic damage models. Most notably, the formulation of localized evolution equations (shear stress/crack displacement law) of the shear response of the crack arises naturally in the proposed framework.

The general framework described in this last item has been developed in Section 3.4 (see also the summary in Table 4.2), with the numerical simulations presented in Section 5 based on the Mode I model (3.50) and a constant degraded shear stiffness. The numerical integration of the general localized multi-surface damage model (3.47) requires additional considerations and will be the subject of a forthcoming publication.

Acknowledgments

I am indebted to L.S. Li for helpful comments while reviewing this manuscript. The numerical simulations presented in Section 4 were obtained with FEAP, courtesy of Prof. R.L. Taylor. Financial support for this research has been provided by the ONR under contract no. N00014-96-1-0818 with UC Berkeley. This support is gratefully acknowledged.

References

- ARMERO, F. [1997] "Localized Anisotropic Damage of Brittle Materials," *Proc. COMPLAS V*, eds. D.R.J. Owen, E. Onate, and E. Hinton, CIMNE, Barcelona.
- ARMERO, F. & GARIKIPATI, K. [1995] "Recent Advances in the Analysis and Numerical Simulation of Strain Localization in Inelastic Solids," *Proc. COMPLAS IV*, eds. D.R.J. Owen, E. Onate, and E. Hinton, CIMNE, Barcelona.
- ARMERO, F. & GARIKIPATI, K. [1996] "An Analysis of Strong Discontinuities in Multiplicative Finite Strain Plasticity and their Relation with the Numerical Simulation of Strain Localization in Solids," *Int. J. Solids and Structures*, **33**, 2863-2885.
- BARENBLAT, G.I. [1962] "The Mathematical Theory of Equilibrium Cracks in Brittle Fracture," *Advances in Applied Mechanics*, **7**, 55-129.
- BAZANT, Z.P.; BELYTSCHKO, M. & CHANG, T.P. [1984] "Continuum Theory for Strain-Softening", *J. Eng. Mech., ASCE*, **110**, 1666-1691.

- BAZANT & OH [1983] "Crack Band Theory for Fracture of Concrete," *Materials and Structures*, RILEM, **16**, 155-177.
- DEBORST, R. & SLYS, L.J. [1991] "Localization in a Cosserat Continuum under Static and Loading Conditions", *Comp. Meth. Appl. Mech. Eng.*, **90**, 805-827.
- COLEMAN, B.D. & HODGON, M.L. [1985] "On Shear Bands in Ductile Materials", *Arch. Rat. Mech. Anal.*, **90**, 219-247.
- CORDEBOIS, J. & SIDOROFF, F. [1982] "Endommagement anisotrope", *J. Mécanique Theor. Appl.*, spécial.
- DUGDALE, D.S. [1960] "Yielding of Steel Sheets Containing Slits," *J. Mech. Phys. Solids*, **8**, 100-104.
- DVORKIN, E.; CUITIÑO, A. & GOIA, G. [1990] "Finite Elements with Displacement Interpolated Embedded Localization Lines Insensitive to Mesh and Distortions," *Int. J. Num. Meth. Eng.*, **30**, 541-564.
- FISH & BELSKY, [1995] "Multigrid Method for Periodic Heterogeneous Media. Part 1: Convergence Studies for One-Dimensional Case. Part 2: Multiscale Modeling and Quality Control in the Multidimensional Case," *Comp. Meth. Appl. Mech. Eng.*, **126**, 1-38.
- GOVINDJEE, S.; KAY, G.J. & SIMO, J.C. [1995] "Anisotropic Modeling and Numerical Simulation of Brittle Damage in Concrete," *Int. J. Num. Meth. Eng.*, **38**, 3611-33.
- HILL, R. [1962] "Acceleration Waves in Solids," *J. Mech. Phys. Solids*, **16**, 1-10.
- HILLERBORG, A.; MODEER, M. & PETERSSON, P. [1976] "Analysis of Crack Formation and Crack Growth in Concrete by Means of Fracture Mechanics and Finite Elements," *Cement and Concrete Research*, **6**, 773-782.
- HILLERBORG, A. [1984] "Numerical Methods to Simulate Softening and Fracture of Concrete," in *Fracture Mechanics of Concrete: Material Characterization and Testing*, eds A. Carpinteri and A. Ingrassia, Marinus Nijhoff Publishers, 141-170.
- PIJAUDIER-CABOT, G.; BODE, L. & HUERTA, A. [1995] "Arbitrary Lagrangian-Eulerian Finite Element Analysis of Strain Localization in Transient Problems," *Int. J. Numer. Meth. Eng.*, **38**, 4171-4191.
- HUGHES, T.J.R. [1996] "Multiscale Phenomena: Green's Function, the Dirichlet-to-Neumann Formulation, Subgrid Scale Models, Bubbles and the Origin of the Stabilized Methods," *Computer Methods in Applied Mechanics and Engineering*, **127**, 387-401.
- JOHNSON, C. [1976] "Existence Theorems for Plasticity Problems," *J. Math. Pures et Appliq.* **55**, 431-444.
- JOHNSON, C. [1978] "On Plasticity with Hardening," *Journal of Mathematical Analysis*

and Applications, **62**, 325-336.

- KACHANOV, L.M. [1986] *Introduction to Continuum Damage Mechanics*, Martinus Nijhoff Publishers, Dordrecht.
- KROPLIN, B. & WEIHE, S. [1997] "Constitutive and Geometrical Aspects of Fracture Induced Anisotropy," *Proc. COMPLAS V*, eds. D.R.J. Owen, E. Onate, and E. Hinton, CIMNE, Barcelona.
- LARSSON, R. & RUNESSON, K. [1996] "Element Embedded Localization Band Based on Regularized Displacement Discontinuity", *J. Eng. Mech.*, **122**, 402-411.
- MANDEL, J. [1966] "Conditions de Stabilité et Postulat de Drucker", in *Rheology and Soli Mechanics*, IUTAM Symposium, Grenoble 1964, ed. by J. Kravtchenko and P.M. Sirieys, 58-68.
- MARSDEN J.E. & HUGHES, T.J.R. [1983] *Mathematical Foundations of Elasticity*, Prentice Hall, Englewood Cliffs.
- MATTHIES, H.; STRANG, G. & CHRISTIANSEN, E. [1979] "The Saddle Point of a Differential Program," in *Energy Methods in Finite Element Analyses*, edited by Glowinski, Rodin & Zienkiewicz, John Wiley & Sons, London.
- NEILSEN, M.K. & SCHREYER, H.L. [1993] "Bifurcation in Elastic-Plastic Materials," *Int. J. Solids Struct.*, **30**, 521-544.
- OLIVER, J. [1989] "A Consistent Characteristic Length for Smeared Cracking Problems", *Int. J. Num. Meth. Eng.*, **28**, 461-474.
- OLIVER, J. [1996] "Modelling Strong Discontinuities in Solid Mechanics via Strain Softening Constitutive Equations. Part 1: Fundamentals. Part 2: Numerical Simulation," *Int. J. Num. Meth. Eng.*, **39**, 3575-3623.
- ORTIZ, M. [1985] "A Constitutive Theory for the Inelastic Behavior of Concrete," *Mech. Mat.*, **4**, 67-93.
- OTTOSEN, N.S. & RUNESSON, K. [1991] "Properties of Discontinuous Bifurcation Solutions in Elasto-Plasticity," *Int. J. Solids Struct.*, **27**, 401-421.
- PETERSSON P.E. [1984] "Crack Growth and Development of the Fracture Zones in Plain Concrete and Similar Materials," Div. Building Mat., Univ. Lund, Rep. TVBM-1006.
- PIETRUSZCZAK, ST. & MRÓZ, Z. [1981] "Finite Element Analysis of Deformation of Strain-Softening Materials," *Int. J. Numer. Meth. Eng.*, **17**, 327-334.
- REINHARDT [1984] "Fracture Mechanics of an Elastic Softening Material Like Concrete," *Heron*, **29**.
- REDDY, B.D. & SIMO, J.C. [1995] "Stability and Convergence of a Class of Enhanced

- Strain Methods," *SIAM, J. Numer. Analysis*, **6**, 1705-28.
- RICE, J. [1976] "The Localization of Plastic Deformations", in *Theoretical and Applied Mechanics*, ed. by W.T. Koiter, 207-219.
- ROTS, J.G.; NAUTA, P.; KUSTERS, G. & BLAAUWENDRAA, T. [1985] "Smearred Crack Approach and Fracture Localization in Concrete," *Heron*, **30**.
- ROYDEN, H.L. [1988] *Real Analysis*, Macmillan Publishing Company.
- SIMO, J.C. & HUGHES, T.J.R. [1997] *Plasticity and Viscoplasticity, Formulation and Numerical Analysis*, Springer Verlag, preprint.
- SIMO, J.C. & JU, J.W. [1987] "Strain- and Stress-Based Continuum Damage Models. Part I: Formulation. Part II: Computational Aspects," *Int. J. Solids Structures*, **23**, 821-840 and 841-869.
- SIMO, J.C; OLIVER, J. & ARMERO, F. [1993] "An Analysis of Strong Discontinuities Induced by Softening Solutions in Rate Independent Solids," *J. Comput. Mech.*, **12**, 277-296.
- SIMO, J.C. & RIFAI, S. [1990] "A Class of Mixed Assumed Strain Methods and the Method of Incompatible Modes," *Int. J. Num. Meth. Eng.*, **29**, 1595-1638.
- SLUYS, L.J. [1997] "Discontinuous Modelling of Shear Banding" *Proc. COMPLAS V*, eds. D.R.J. Owen, E. Onate, and E. Hinton, CIMNE, Barcelona.
- STAKGOLD, I. [1979] *Green's Functions and Boundary Value Problems*, Wiley, New York.
- SUQUET, P.M. [1981] "Sur les Equations de la Plasticité: Existence et Régularité des Solutions," *Journal de Mécanique*, **20**, 3-39.
- TRUESDELL & NOLL [1965] "The Nonlinear Field Theories of Mechanics," *Handbich der Physik Bd. III/3*, ed. by S. Fluegge, Springer Verlag, Berlin.
- DE VITO, L. [1966] "Fondamenti della Meccanica dei Sistemi Continui," in *C.I.M.E., Non-linear Continuum Theories*, 19-104, ed by. G. Grioli & C. Truesdell, Cremonese, Rome.